AE4020 Literature Review

Review of Laser-Thermal Propulsion Literature

Presented to Ir. B.T.C. Zandbergen

Emmanuel Duplay
5468515
MSc. Aerospace Engineering
Space Track
Space Exploration Profile

December 13, 2022

TU Delft

McGill

Contents

List of Figures

List of Tables

Nomenclature

Abbreviations

CW	Continuous-Wave
DE	Directed-Energy
DEP	Directed-Energy Propulsion
HET	Hall-Effect Thruster
IB	Inverse Brehmsstrahlung
LEP	Laser-Electric Propulsion
LSC	Laser-Supported Combustion
LSP	Laser-Sustained Plasma
LTP	Laser-Thermal Propulsion
OTV	Orbital Transfer Vehicle
RP	Repetitively-Pulsed

Latin symbols

c	Speed of light in a vacuum (2.998×10^8 m/s)
c_D	Damping factor
D	Diameter
d	Distance
F	Force
g_0	Standard gravity (9.80665 m/s^2)
I	Local laser flux [W/m^2]
I_sp	Specific impulse [s]
k	Stiffness
k_L	Radiation absorption factor [1/m]
m	Mass
$\dot{m}$	Mass flow rate
$\mathscr{M}$	Molar mass
P	Power
p	Pressure
R_u	Gas constant, universal (8.31446 J/K mol)
R_g	Gas constant, specific
T	Temperature
v	Velocity
x	Displacement

Greek symbols

α	Absorption factor
ϵ_r	Reflectivity
ζ	Damping ratio
η	Efficiency
θ	Divergence angle
κ	Conductivity
λ	Wavelength
ρ	Density
ω	Frequency

Subscripts

c	Thrust chamber
d	Damping
e	Laser emitter
ex	Exhaust
f	Focusing length
n	Natural (frequency)
R	Rayleigh range
r	Laser receiver
T	Thrust

Chapter 1

Introduction

The long-term settlement of other planetary bodies will likely demand the development of high-efficiency, high-thrust propulsion technologies to facilitate crew and cargo transportation across the solar system. This research project will investigate one potential candidate: laser-thermal propulsion (LTP). A broad overview of the concept will be given in this chapter, along with the definition of research objectives and research questions to be answered in this literature review and a follow-on thesis project.

1.1 Context and Motivation

Despite the recent progress made by the commercial space sector in facilitating access to Earth orbit, space travel beyond Earth's sphere of influence has remained largely unchanged in terms of transit time and propulsion technologies, particularly for crewed missions. Although small robotic missions can use highly-efficient electric propulsion to explore deep space, humans will still use chemical propulsion to go to Mars, with propellant combinations that have been known for decades. Unfortunately, these propellants have a low fundamental limit to the specific impulse that they can deliver in a rocket motor, often limiting the capabilities of these propulsion systems to small payloads and long mission times, or requiring multiple launches and in-space refueling to deliver larger payloads. If humanity is to settle other worlds in the solar system, alternate propulsion systems with greater specific impulse yet moderate/high thrust will be needed, to enable flexible, rapid transit across the solar system.

One such alternate propulsion system is laser-thermal propulsion, wherein a propellant (e.g., hydrogen gas) is directly heated in a thrust chamber with a high-power laser through a mechanism called laser-sustained plasma (LSP) or laser-supported combustion[1] (LSC): focused laser radiation reaches intensities sufficient to dissociate and ionize the propellant, sustaining a small (relative to surrounding gas) plasma core. This laser would be beamed from a remote emitter, either on the ground or aboard an orbiting station, with the necessary power generation, storage and delivery capacity. Using a laser (or directed-energy (DE)) instead of a chemical reaction to heat the propellant has two advantages:

1. Offloading part of the spacecraft's power and propulsion system mass to the ground reduces the spacecraft's dry mass, providing a greater allowance for payload and/or

[1] In this case, no actual combustion occurs, but the dynamics are analogous

propellant.

2. The thrust chamber temperature, a key driver of specific impulse, is now decoupled from propellant chemistry (Nored [1]). As long as enough power is available, the chamber temperature can be raised to the thermo-mechanical limits of the chamber walls, maximizing the specific impulse delivered by the thruster.

LTP was the subject of significant research efforts in the 1970s and 1980s for launch vehicle and orbital tug applications, as the range of available high-power lasers was limited to Low-Earth Orbit. This interest unfortunately waned as the Cold War drew down—the Strategic Defense Initiative missile defense program not only considered lasers to destroy ICBMs, but also supported research on their application to propulsion (Kare [2]), and many experiments relied on military facilities (Myrabo [3] and Black *et al.* [4]).

Today, new laser technologies developed for the telecommunications industry enable the practical realization of the large laser arrays required for directed-energy propulsion. Indeed, fiber-optic lasers can be phase-locked together to act as a single optical element, allowing the modular and inexpensive construction of large laser arrays, as discussed for interstellar flight applications by Lubin [5]. The shorter wavelength (1.06 micron) and ability to construct meter- to kilometer-scale arrays expands the applications of directed-energy propulsion to interplanetary missions. In the case of LTP, its theoretical thrust and specific impulse would allow fast interplanetary transits for crewed missions, minimizing astronauts' exposure to radiation hazards such as galactic cosmic rays or solar particle events. Alternatively, slow missions could benefit from a considerable payload capacity, facilitating the settlement of other planets, as discussed by Duplay *et al.* [6].

1.2 Research and literature review goals

The potential benefits of laser-thermal propulsion and the renewed interest in DE propulsion warrants revisiting the experimental and theoretical research done on LTP and LSP. This literature study will explore the past work done on the topic to determine the latest state of research, gain insight on the challenges encountered and whether they can be overcome thanks to recent technology developments. Laser-thermal propulsion will also be compared to alternative propulsion systems to determine whether it provides compelling advantages. Past TU Delft students have investigated an analogous propulsion system using the sun as a heat source (solar-thermal propulsion), so special attention to the work done by Takken [7] will be given as a form of comparison.

The main research objective of this thesis project would be to *reproduce past LSP experiments by designing an experimental LTP thruster with current-day fiber laser technology*. At the most basic level, the following research questions are relevant to the objective:

- What impact, if any, does the use of a 1.06-μm-wavelength fiber laser versus a 10.6 μm CO_2 laser have on the LSP mechanism or the performance of the thruster?
- How can the thrust performance be improved compared to past experiments?

These research objectives and questions can and likely will evolve through this literature review, which will focus on several aspects of laser-thermal propulsion. First, the parent field of directed-energy propulsion will be reviewed, as it provides context for the emergence of LTP, and is necessary to discriminate between several types of laser propulsion.

This chapter will also discuss the advantages and challenges relevant to DEP architectures, and some fundamental aspects of laser physics.

Chapter 3 will then provide an in-depth discussion of laser-thermal propulsion, specifically laser-plasma propulsion (as LTP can refer to several different concepts). The specific niche of LTP will be identified and contrasted with other propulsion systems, such nuclear-thermal propulsion and laser-electric propulsion. Potential applications will be explored, and key engineering challenges in implementing the concept will be investigated. The key energy conversion mechanism involved in LTP, *laser-supported plasma*, will also be discussed. This review will consider both the theoretical modelling and experimental work done since the inception of the field. Specific attention will be given to the laser absorption processes and radiative heat transfer mechanisms, as these will strongly influence the performance of the LTP thruster.

Finally, Chapter 4 will consider the practical matters of creating an experimental setup for the study of LTP. This will cover aspects of the research that may be specific to LTP, as informed by past experimental work, and aspects that are generally shared with thruster experiments, such as the design of a thrust stand and required instrumentation. Together with Chapter 3, this chapter will attempt to determine existing research gaps in LSP research and LTP thruster development.

Chapter 2

Directed-Energy Propulsion

Directed-Energy Propulsion (DEP) refers to a type of propulsion where the energy used to propel a vehicle is not stored onboard (such as in a fuel tank or a battery), but instead is provided remotely and wirelessly, typically by electromagnetic radiation. The main advantage of this family of propulsion concepts is the reduction in mass associated with power and propulsion subsystems, and for some types of DEP, can bypass the challenges imposed by the rocket equation altogether.

This chapter will provide an overview of the field of DEP, briefly describing energy transfer mechanisms, notable concepts for space propulsion, and discussing the architecture-level challenges specifically associated with laser space propulsion systems.

2.1 Laser physics

Due to the distances and the media (or lack thereof) through which energy must be transmitted for space propulsion, DEP uses electromagnetic radiation to deliver power to a spacecraft. Specifically, coherent beams of radiation (i.e., lasers or masers) are typically preferred, as their low beam divergence maximizes the operational range of DEP systems. Conventional radiation sources would be unable to concentrate their power on a spacecraft, and most of the emitted power would be lost.

In order to assess the performance and capabilities of DEP systems, some fundamental understanding of optics (or photonics) is necessary. Discussion will focus on lasers, as they are more common in the literature and are used for laser-thermal propulsion. That said, most concepts will still apply to masers, as they are just a different wavelength of electromagnetic waves. Hecht [8] provides a an overview of laser physics and photonics, discussing both the mechanisms of light amplification, and the optical behavior of laser beams. The relevant aspects of laser physics as described by Hecht are summarized below.

The key property of laser beams is the *coherence* of their light waves. Most sources of light emits waves across a broad spectrum of wavelengths and out of phase. Their beams (e.g., out of a regular flashlight) are greatly affected by diffraction, and their beam diameter spreads out significantly over a short distance. Lasers, thanks to the mechanism of stimulated emission, emit light waves in a narrow range of wavelengths and almost perfectly in-phase. This is illustrated in Figure 2.1. This coherence allows laser beams to exhibit a low divergence angle, i.e., they appear to form a beam of constant diameter, unlike light beams from the sun or artificial lighting.

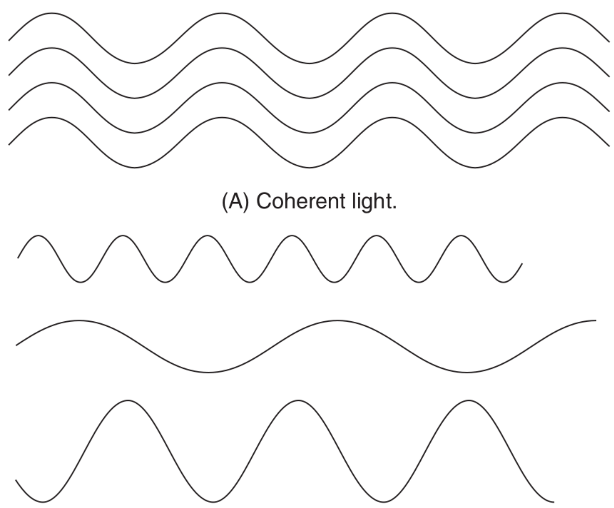

(A) Coherent light.

(B) Incoherent light.

Figure 2.1: Coherence of light waves, from Hecht [8]

Nevertheless, although laser beams appear as straight narrow beams, they are still subjected to diffraction, and do eventually spread out, though at a much lower rate than incoherent light. The anatomy of a laser beam is shown in Figure 2.2. A portion of the beam leaving the emitter is in the *near-field*, where light waves are parallel and the beam exhibits little to no divergence—the length of this portion is called the *Rayleigh range* d_R, defined in Equation 2.1, where D_e is the emitter's aperture diameter and λ is the wavelength of the laser.

$$d_\mathrm{R} = \frac{D_\mathrm{e}^2}{\lambda} \tag{2.1}$$

Beyond the Rayleigh range, in the *far-field*, light waves begin to measurably spread out, as quantified by the divergence angle θ of the beam. This divergence angle is also a function of the emitter's aperture size and the laser wavelength, as seen in Equation 2.2. It is additionally scaled by a constant K, whose value depends of the profile of the beam, i.e., the distribution of power across the beam's cross-section. For a uniform cross-section, $K = 1.22$, but for most laser beams, the profile has a peak intensity at the center of the beam, and smoothly falls off towards the edges, and $K \approx 1$ in this case.

$$\theta = \frac{K\lambda}{D_\mathrm{e}} \tag{2.2}$$

The beam diameter in the far field can then be calculated by trigonometry. This raises the question of how the beam diameter is defined in the first place. As mentioned above, the beam profile of most lasers is a smooth function, with the intensity approaching zero away from the centerline of the beam. In fact, the ideal laser beam profile is Gaussian: the intensity follows a normal distribution, with the peak intensity reached in the middle of the cross-section. Since a normal distribution never reaches zero, there is no natural "edge" to the beam, and the diameter thus has several definitions. Most commonly, the $1/\mathrm{e}^2$ definition is used, referring to the width of the beam profile where the intensity is greater than $I_\mathrm{max}/\mathrm{e}^2$, or 13.5% of the maximum intensity.

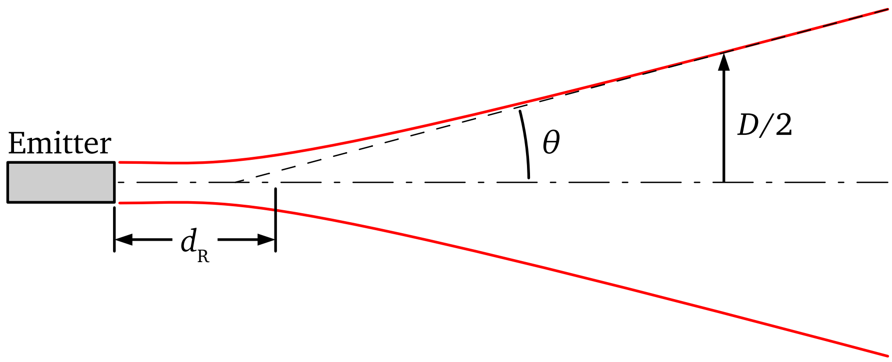

Figure 2.2: Gaussian laser beam geometry

The final aspect of beam anatomy of particular relevance to directed-energy propulsion is the focusing distance of a laser beam. Indeed, as DEP concepts involve the transmission of energy to a spacecraft over long distance, this focusing limit is important to determine power losses and the required size of laser receivers aboard the spacecraft. Thankfully, the relationship between these parameters is captured quite simply in Equation 2.3.

$$d_\mathrm{f} = \frac{D_\mathrm{e} D_\mathrm{r}}{\lambda} \tag{2.3}$$

The distance d_f at which a laser emitter of diameter D_e is capable of focusing a spot of diameter D_r is proportional to both diameters, and inversely proportional to the wavelength of the laser beam. This equation is given by Hecht [8], and is also seen in a paper by Lubin [5] describing a comprehensive DEP architecture for interstellar flight. Depending on the beam diameter definition used, a scaling factor may be included in the equation.

2.2 Applications of DEP for spacecraft

DEP encompasses a wide range of propulsion concepts, as the directed energy received by the targeted spacecraft can be converted into momentum through numerous direct and indirect ways.

Lightsails Identical to solar sails in operating principle, lightsails differ only in their source of light. Photons carry momentum, and can transfer it to an object when reflected. Urbanczyk [9] provides an overview of the mathematics governing solar sail propulsion, highlighting that the concept had been proposed as early as the 1920s by Konstantin Tsiolkovsky. Radiation pressure is now a well-understood concept: it has been used on several solar sail demonstrator missions such as JAXA's IKAROS (Mori *et al.* [10]), and is often taken into account for trajectory planning of conventional spacecraft. In the case of DEP lightsails, the mechanics are generally the same—assuming the entire beam is incident on a sail of reflectivity ϵ_r, a laser of power P will apply a force F to the sail as given by Lubin [5]:

$$F = \frac{P(1-\epsilon_r)}{c} \tag{2.4}$$

Where c is the speed of light. This force is always exerted normal to the incident surface, much like the momentum transfer of a ball bouncing on a plane. As opposed to solar sails, given a laser array of sufficient power and a sail of low enough mass, relativistic speeds could be practically achieved, so relativistic effects of apparent mass increase must be considered as well. This is also discussed by Lubin [5], who is a major proponent of the use of DEP lightsails for near-term interstellar missions. Indeed, as this propulsion method does not throw away mass to accelerate, it is not subject to the rocket equation. Lubin and Hettel [11] suggest that gram-scale spacecraft could conceivably be accelerated enough to reach the closest star system (Alpha Centauri) in a few decades. No known rocket propulsion system, even at the lowest TRL, would be capable of this feat. However, although such a system could be used for interplanetary flight applications, the required laser arrays would be of even greater power for any useful mission, making this concept impractical compared the some of the following alternatives.

Laser-electric propulsion Instead of using direct radiation pressure, laser energy can instead be converted to electricity using photovoltaic (PV) cells, to then power electric propulsion systems, such as gridded ion engines or Hall-effect thrusters. This is the concept of laser-electric propulsion (LEP). The architecture proposed by Brophy *et al.* [12] and Sheerin *et al.* [13] applies principally to rapid interplanetary flights, with continuous thrust provided by gridded ion engines. Using lasers to power these systems come with several advantages. First, the power level available to the spacecraft can be much greater than for conventional electrically-propelled vehicles, which often only rely on solar power alone. As seen in Equation 2.7, derived from rocket motor theory (Zandbergen [14]) by relating the input laser power P_{in} to jet power P_{jet}, increased power allows for a much greater level of thrust F_{T} and/or exhaust velocity v_{ex}, enabling faster missions.

$$F_{\text{T}} = \dot{m} v_{\text{ex}} \tag{2.5}$$

$$P_{\text{in}} = \frac{P_{\text{jet}}}{\eta} = \frac{\dot{m} v_{\text{ex}}^2}{2\eta} \tag{2.6}$$

$$\implies P_{\text{in}} = \frac{F_{\text{T}} v_{\text{ex}}}{2\eta} \tag{2.7}$$

Second, as lasers are monochromatic, the PV cells can be tuned to be most efficient at the laser's wavelength, reducing the required PV mass for a desired power: while the best experimental solar cells, such as the ones developed by Geisz *et al.* [15], have yet to breach the 50% efficiency mark, tuned monochromatic PV cells are now almost 70% efficient (Helmers *et al.* [16]).

LEP has a few disadvantages. Notably, while the available power is far greater than its solar-powered counterpart, it is still a typically low-thrust system, with propulsion durations spanning days and weeks for many missions. This is not necessarily an issue for solar-electric systems, but in the case of LEP, a laser array must be able to provide power continuously throughout the propulsive maneuver. LEP missions such as the ones proposed by Sheerin *et al.* [13] thus require significant DEP infrastructure:

1. Continuous low-thrust missions will typically mean that the distance between the spacecraft and the laser array will be large. By Equation 2.3, the laser array and the spacecraft's PV array must thus be quite large as well. As reported by Sheerin *et al.* [13], such arrays will often be comparable in size to those needed for interstellar propulsion ($\sim$1 km).
2. Since a laser link must be maintained for several days to months, a single ground-based laser array is not sufficient for many LEP missions. Several arrays must be built

around the planet to ensure constant power transmission. Alternatively, such a laser array must be constructed in-orbit, which comes with additional technological and political challenges.

In addition, PV cells are quite sensitive to incident radiation compared to the thin dielectric reflectors considered for interstellar missions. Sheerin *et al.* [13] considered a 10 kW/m^2 limit on the irradiance of PV cells with passive cooling, which is several orders of magnitude less than the irradiance considered by Lubin [5] for interstellar lightsails. This constraint will force LEP systems to use larger and heavier PV arrays, reducing their power-to-mass ratio (specific power).

Laser-thermal propulsion Laser-thermal propulsion (LTP) encompasses several different laser propulsion concepts where the laser energy is used to thermally energize a propellant. Kantrowitz [17] first proposed this concept as a means to reduce launch costs to orbit. Mori [18], Eckel and Schall [19], and Myrabo [20] discuss several different LTP concepts, which can be categorized based on the laser regime considered (repetitively-pulsed (RP) versus continuous-wave (CW)), and the energy conversion mechanism used to convert laser power into enthalpy:

- *Pulse-detonation* (RP) Pulse-detonation engines use high power laser pulses to detonate propellant, which can be in solid or gaseous phase. This form of propulsion includes laser-ablation propulsion when using sold fuels. The most notable work done on such a concept is Myrabo [3]'s Lightcraft demonstrator—an air-breathing pulse-detonation craft which reached a height of 71 m in 2000, powered by a 10-kW CO_2 pulse laser. The craft uses a specially designed spike nozzle that focuses incoming laser radiation onto air flowing through the vehicle. Meloney *et al.* [21] have studied a variant of this concept using a maser (microwave laser) to provide power, with the additional benefit of powering a magnetohydrodynamic (MHD) drive to augment the craft's thrust.
- *Heat-exchanger* (CW) Proposed by Kare [22], laser-heat-exchanger propulsion is similar in many respects to solar-thermal propulsion, where the incident radiation's energy is focused onto a heat-exchanger through which the propellant flows. The use of laser power allows for much greater power levels than solar-thermal propulsion, but the specific impulse is limited to 900 s according to Mori [18], due to the thermal limits of the heat-exchanger's materials.
- *Laser-plasma* (CW) Keefer *et al.* [23] provide a detailed review of laser-plasma propulsion. This concept considers a continuous laser used to sustain a plasma core (laser-sustained plasma, LSP) in a thrust chamber. This plasma serves as the energy conversion mechanism from laser radiation to heat, and energizes the surrounding propellant. Thanks to this more direct conversion method, laser-plasma propulsion is theoretically able to achieve much greater exhaust velocities ($I_{sp} \geq 1000$ s) than heat-exchanger concepts. This is the propulsion concept that will be studied in-depth for this literature review and follow-on thesis project, and will be referred to as laser-thermal propulsion in the following chapters.

Research interest in these LTP implementations generally considered launch vehicle and Orbital-Transfer Vehicle (OTV) applications: The seminal talk on laser propulsion given by Kantrowitz [17] is motivated by a need for lower launch costs, Mori [18] and Kare [22] focus primarily on launch vehicle design and trajectories. In particular, Kare argues that laser-heat-exchanger rockets are well suited for launch purposes (as opposed to laser-plasma and pulsed propulsion) as they do not require complex onboard opto-mechanics to redirect and focus the laser beam; it need only be incident on the heat-exchanger surface. Mori [18] concurs, suggesting that the Very Small Launch Vehicle (VSLV, dedicated launch of 1–10 kg payloads) market is an attractive niche for laser-propulsion launchers with emitter powers on the order of several megawatts.

Alternatively, the potential availability of high-power, large-aperture laser systems enables interplanetary transit applications. As such missions deal with fewer losses to gravity and drag, much larger payloads can be injected to interplanetary transfer orbits with MW-class arrays, provided that they are placed in Earth orbit by conventional launchers (Duplay *et al.* [6]).

2.3 Laser propulsion architecture

Although the methods to convert laser power into momentum vary greatly between the concepts above, they do share a commonality on the need for large, powerful laser systems. Earlier work on directed-energy propulsion often considered the use of free-electron lasers (Myrabo [20], illustrated in Figure 2.3a) or carbon-dioxide lasers (Eckel and Schall [19]), as they were prime candidates for laser technologies capable of providing the required power and wavelengths for DEP. However, Lubin [5] proposes an alternative architecture leveraging the development of fiber lasers for the telecommunications industry. Lubin argues that their massive commercial use has driven down their cost and their complexity to a point where large-scale, high power laser arrays can be constructed more practically than with alternative laser technologies. Furthermore, using a Master Oscillator Power Amplifier (MOPA) architecture allows for a progressive development of the necessary infrastructure. This highly-attractive concept has led to a renewal of the study of DEP concepts, leading to many recent studies assuming the use of fiber laser arrays (as shown in Figure 2.3b) operating at the 1064-nm wavelength—this near-infrared light is able to traverse the atmosphere with practically no losses due to absorption (Gemini Observatory [24]).

Ensuring reliable transmission and focus through the atmosphere is a critical requirement of ground-based laser arrays, but the high transparency of the atmosphere is not sufficient to guarantee this. Turbulence and localized temperature gradients in the atmosphere change the way light is refracted, which would likely reduce the laser beam quality by the time it reaches space. This effect can be observed when looking at the night sky—stars twinkle due to these disturbances. Since astronomers do most of their work using ground-based telescopes, this issue has led them to develop adaptive optics. These optics are able to adjust to atmospheric conditions in real-time to correct for disturbances. The same technology can be used in the reverse direction for DEP. In fact, Eckel and Schall [19] go as far as saying that "the problem of adaptive optics can be considered as being technologically solved." Furthermore, Hettel *et al.* [26] have performed a comprehensive numerical simulation of beam propagation from a laser array using realistic system noise and turbulence models, showing that such systems could produce diffraction-limited spots—i.e., they are limited by Equation 2.3—in outer space for zenith angles of less than 60°. These studies provide confidence in the feasibility of laser power transmission through the atmosphere.

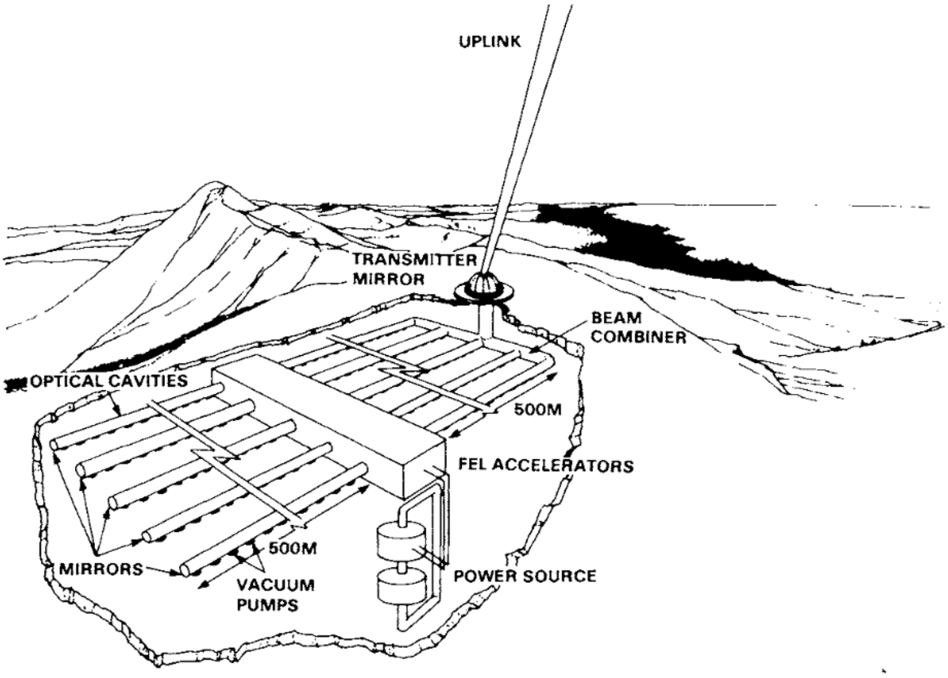

(a) Free electron laser facility for DEP, as imagined in 1984 by Myrabo [20]

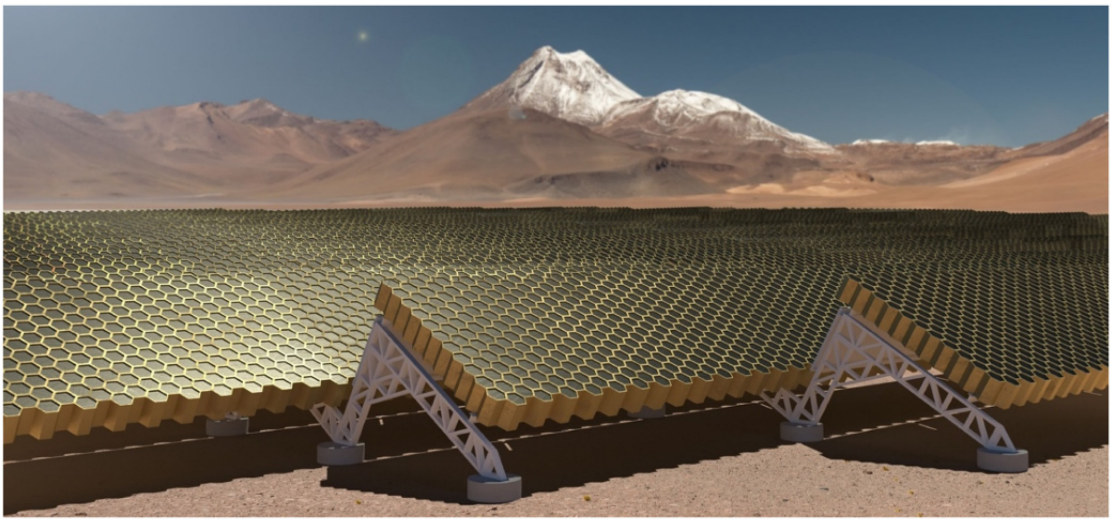

(b) Fiber laser array for interstellar propulsion, as conceptualized in 2021 by Worden *et al.* [25]

Figure 2.3: Evolution of ground-based laser array architecture

Chapter 3

Laser-Thermal Propulsion

Laser-thermal propulsion, specifically laser-plasma propulsion, provides the most effective means of converting continuous laser radiation into heat within a propellant. Proposed by Nored [1] in 1976, its theoretical specific impulse of 1000 s to 3000 s greatly exceeds the capabilities of chemical rocket engines and competes with many nuclear-thermal propulsion concepts. This chapter will discuss the LTP concept in general, how it compares to alternative propulsion systems, and the physical mechanism at its (literal) core: laser-sustained plasma (LSP).

3.1 Concept

LTP uses incoming laser radiation to energize gaseous propellant and generate thrust within a thermal rocket motor. Its operation and design is similar to chemical or nuclear-thermal propulsion systems, with a major difference in the heat generation mechanism. The laser radiation powering LTP is focused into a thrust chamber, increasing the local irradiance of the laser enough to sustain a plasma core in the flowing propellant. This plasma is critical to the operation of the thruster, as serves as the conversion mechanism from laser radiation to heat in the propellant.

As alluded to in the Introduction, the key advantage of laser-thermal propulsion over chemical propulsion is its ability to deliver far greater exhaust velocities. Following from thermal rocket theory (Zandbergen [14]), the exhaust velocity v_{ex} of a thermal rocket motor depends on Equation 3.1, where γ is the specific heat ratio of the propellant gas, R_{u} is the universal gas constant, $\mathscr{M}$ is the propellant molar mass, and T_{c} is the chamber temperature.

$$I_{\mathrm{sp}} g_0 = v_{\mathrm{ex}} \propto \sqrt{2 \frac{\gamma}{\gamma - 1} \frac{R_{\mathrm{u}}}{\mathscr{M}} T_{\mathrm{c}}} \tag{3.1}$$

This equation suggests that for two rocket motors operating at the same pressure ratio, the one operating at the higher temperature will have a greater specific impulse. In chemical propulsion systems, this chamber temperature is limited to the chemical reaction's adiabatic flame temperature. Chemical rockets have long attained this limit: the best performing propellant combination (Lithium-Fluorine-Hydrogen) achieved just over 500 s of specific impulse in tests performed by Arbit *et al.* [27] in 1970, but found little practical use. The RL10 hydrogen/oxygen vacuum engine is the best performing rocket engine used in practice, with a maximum specific impulse of 465.5 s [28]. Externally-heated rocket thrusters are not subjected to adiabatic flame temperature limits, and are thus capable of delivering much greater exhaust velocities. An added bonus of external heating is that pure hydrogen does not need to be mixed with an oxidizer, which would increase the exhaust's molar mass and thus reduce the exhaust velocity. These advantages are true for nuclear-thermal propulsion, laser-heat-exchanger rockets, and laser-plasma rockets (LTP).

However, the direct coupling of the laser radiation to the propellant in LTP comes with a few additional advantages over other forms of externally-powered propulsion systems:

- The incident laser irradiance on the spacecraft's receiver is no longer constrained by the low thermal limits of power conversion systems, such as photovoltaic cells or heat exchangers. Reflective optics are generally more robust and efficient than PV—"arbitrarily high" reflectivity can be achieved using layers of dielectric materials, as proposed for laser-driven lightsails by Lubin [5].
- The simplicity of the receiving and focusing mirror allows the propulsion system to be lighter than a comparable LEP system or nuclear-thermal system, thanks to the use of inflatable structures, as proposed for solar-thermal propulsion applications (Gerrish [29]).
- The simplicity of this heat addition method further reduces the propulsion system mass compared to liquid bipropellant systems—no mixing or spraying is required.

The flow within the thruster is illustrated in Figure 3.1. As the laser radiation is only absorbed by the plasma, the engine should be designed to ensure high absorption of radiation by the propellant and good mixing of both flows upstream of the nozzle. These issues were identified by Shoji and Larson [30], who performed a thorough analysis of heat transfer within two LTP engines, proposing seeding the flow with carbon particles as a solution to reduce radiative heat losses to the chamber walls. Their analysis showed that such losses could be reduced to 4.5 % of the input laser power.

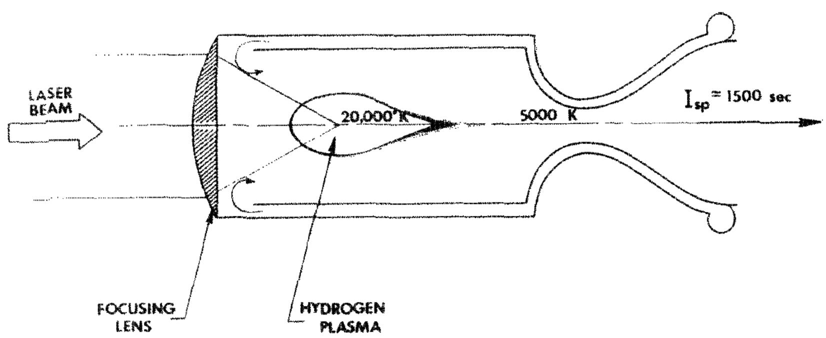

Figure 3.1: Conceptual LTP engine diagram, by Keefer [31]

The operation of such an engine is otherwise similar to other types or thermal rocket engines. The heated gas is accelerated through a supersonic nozzle, expanding it to match the ambient pressure. Cooling of the thrust chamber and nozzle could be done using the same methods as chemical rocket engines, though Nored [1] expressed some doubt about this, as the greater temperatures and radiation-dominated heat transfer encountered in LTP could potentially require more effective solutions. Nored identified several other relevant areas of further research, such as plasma initiation and stability, and the development of robust, low-absorption windows.

3.2 Laser-Sustained Plasma

One might wonder why bother with plasma at all. If the laser radiation could be deposited evenly in the propellant flow, little to no mixing would be needed and peak temperatures would be lower. Unfortunately, the use of lasers to directly heat hydrogen propellant has a major flaw: hydrogen gas does not absorb 1-µm-wavelength radiation at room temperatures. Hydrogen only begins to absorb this wavelength at around 10 000 K, as shown by Glumb and Krier [32]: "The paradox is that hydrogen cannot absorb any laser radiation unless it is already hot." They were considering 10.6 µm laser radiation, but this also holds for 1.06 µm. The reason for this being that this wavelength does not match hydrogen's resonance absorption bands, whereby radiation is absorbed in the rotational or vibrational modes of a molecule. The main absorption mechanism in LSP is *inverse brehmsstrahlung* (IB): free electrons absorb radiation across a continuous spectrum (as opposed to specific wavelengths) during collisions with ions in the plasma (Keefer [31]). Keefer showed that for typical cases where the photon energy is much less than the thermal energy of the plasma, the absorption factor α will vary with the frequency ω of the radiation as follows:

$$\alpha \propto \left(\frac{\pi c}{\omega}\right)^2 \tag{3.2}$$

Since such free electrons are only present once hydrogen has ionized, absorption of 1.06-µm-wavelength radiation by IB can only occur in hydrogen plasma.

While this poses a problem to initiate the LSP process, Raizer [33] theorized that once properly initiated, an LSP wave (also referred to as "light spark", "optical plasmotron", "continuous optical discharge", or "laser-supported combustion wave" in the literature) could be sustained in flowing gas. This was soon confirmed experimentally by Generalov *et al.* [34], who sustained a Xenon plasma using a 150 W CW CO_2 laser. Plasma initiation was performed using a pulsed laser of 10-kW-peak power. Several experimental studies of LSP then followed, using a variety of solutions for plasma initiation, as will be discussed in detail in Section 4.1. In addition to showing the feasibility of LSP, Generalov *et al.* also note that the chamber pressure affects the ease of maintaining an LSP wave: in their experiments, they failed to maintain it below 3 atm, and pressures above 4 atm were too unstable.

Once a plasma is initiated, its shape and position will stabilize at an equilibrium point where the local laser intensity is just sufficient to compensate for thermal losses of the plasma front (Keefer [31]). This state and its stability will be affected by beam geometry and flow conditions (Welle *et al.* [35]). Experiments by Fowler and Smith [36] show that a key aspect of beam geometry is the ratio of the converging beam's focal length to its initial diameter at the focusing lens, known as the f-number, often denoted f/N, where N is the f-number. Low f-numbers—i.e., short focal lengths with a wide initial beam diameter—produce stable plasmas which will remain close to the beam's focal point thanks to the rapid decrease in laser intensity, while the plasmas of high f-number optics will propagate away from the focus (Keefer [31]) and may be too unstable to be maintained continuously: Fowler and Smith have found that optical systems of $f/10$ and greater could not sustain a stable plasma.

Since the first model derived by Raizer, theoretical/numerical models of LSP saw progressive improvements, providing greater insight into the optimal conditions for plasma maintenance and laser absorption. Notably, Jeng and Keefer [37] developed a fully two-dimensional numerical model of hydrogen LSP in 1986 that suggests close to complete laser absorption can be achieved under certain conditions (3 atm of static pressure, 10 kW input power). This model also showed that radial velocity components of the flow were significant, meaning that the one-dimensional or quasi-two-dimensional models developed earlier, such as the one by Batteh and Keefer [38], were unsuitable for the analysis of LSP problems. Jeng and Keefer's model also allowed for the study of the laser wavelength's effect on the resulting plasma, an analysis that was impractical to perform experimentally. Jeng found that due to the gas absorption length's dependence on the applied electric field frequency, reducing the laser wavelength from 10.6 µm to 3.9 µm led to lower absorption rates and longer plasmas along the beam axis, due to the inversely proportional relation seen in Equation 3.2 (Keefer [31]). This is a highly relevant factor to consider for an experiment looking to study LSP using modern fiber lasers operating at 1.06 µm.

Several experiments on laser-sustained plasmas have been performed since Generalov *et al.*'s first plasmotron in 1970. Early studies explored the parameter space for the successful maintenance of LSP, with specific attention given to the ranges of pressures and laser power (threshold power) required. Moody [39] provides a thorough exploration of this parameter space for Argon plasmas sustained by a 10.6 µm laser, showing a $P \propto 1/p^2$ relation between the laser power P and the gas pressure p at < 10 atm, as shown in Figure 3.2a. In his study, the minimum pressure at which an LSP was achieved was 2 atm, for a laser power approaching 300 W. Higher pressures allow for a lower input power, and can enable ambient atmosphere operation of a thruster, greatly simplifying experimental design. Similar experiments have been performed for other gases showed that the threshold power was typically greater for molecular gases such as hydrogen (Keefer [31]).

Another parameter affecting successful LSP maintenance is flow velocity, as shown by the studies of Welle *et al.* [35], Krier *et al.* [40], and Gerasimenko *et al.* [41]. While early experiments were typically performed in static gas, with natural convection being the only source of flow, the effect of forced convective flow was studied both for its benefits to the resulting LSP, and the application of LSP within a laser-thermal thruster. Welle *et al.* varied the flow speed from 0.4 m/s to 4.5 m/s in Argon plasmas sustained by a 1 kW laser, measuring laser absorption and thermal radiation losses. They found that there are optimal pressure and flow speed conditions to maximize laser absorption, and that thermal radiation correlates with laser absorption. For pressures above 1.5 atm, increased flow speed appears to improve absorption compared to the static case. The authors suggest that the flow forced the plasma closer to the high-intensity laser focus, as seen in Figure 3.2b, improving absorption characteristics. In the case of Figure 3.2b, this translated to an improvement from 66 % to 83 %. Gerasimenko *et al.* found that in some cases, forced convection enables the maintenance of LSP under pressure and laser power conditions that would otherwise not allow it.

3.3 Performance

In his overview of applications of lasers for space propulsion, Nored [1] provides some theoretical thrust performance data for laser-thermal propulsion, claiming that specific impulses of 1000–2000 s could be achievable with this concept, as seen in Figure 3.3a. In fact, the propellant mass flow and laser power could be adjusted to raise the specific impulse to even greater values, provided the engine is designed to handle extreme chamber temperatures. Thrust levels can be estimated based on the laser power using Equation 2.7, and is plotted in Figure 3.3b assuming a conversion efficiency of 50 %. This was an arbitrary value selected by Glumb and Krier [32], but is sufficient to illustrate the governing relationship

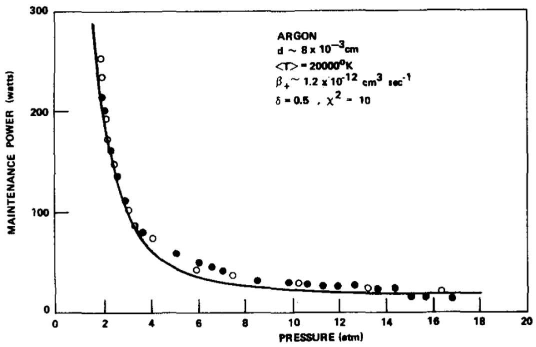

(a) Pressure dependence on required laser input power to maintain LSP in Argon, reproduced from Moody [39]

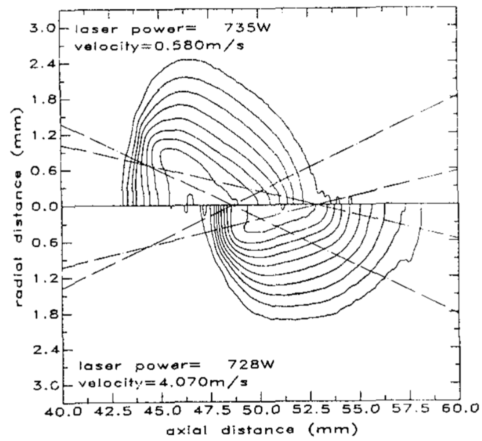

(b) Temperature profile of Argon plasmas at two flow velocities, reproduced from Welle *et al.* [35]. Intervals of 500 K with outer contour at 10 500 K.

Figure 3.2: Dependence of LSP on pressure and flow velocity

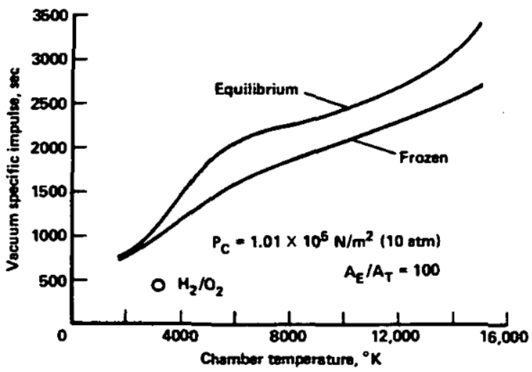

(a) Theoretical specific impulse, Nored [1]. Note the comparison to hydrolox propulsion.

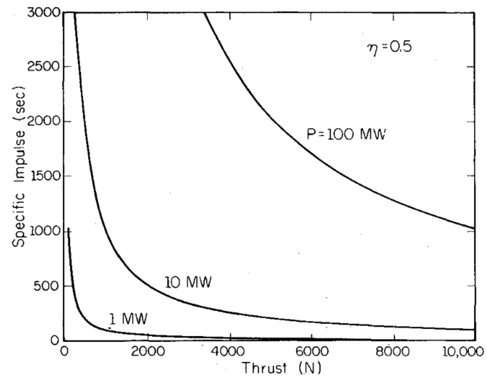

(b) Power vs. thrust, Glumb and Krier [32]

Figure 3.3: LTP performance parameters

between power, thrust, and specific impulse in power-limited rocket propulsion systems. As seen in these plots, the expected thrust delivered by LTP is on the order of several kN for the powers considered using phased-arrays of fiber lasers.

With these performance parameters, LTP can be compared to other conventional or proposed propulsion systems to identify its specific niche. The following propulsion concepts are compared in Figure 3.4:

- Chemical propulsion, represented by the RS-25 [42], RL10 [28], and Raptor 2 Vacuum engines [43]
- Nuclear-Thermal Propulsion (NTP), using 2 test articles from the Rover NTP test program discussed by Koenig [44]
- The proposed VASIMR system, providing a data point for Nuclear-Electric Propulsion (NEP)

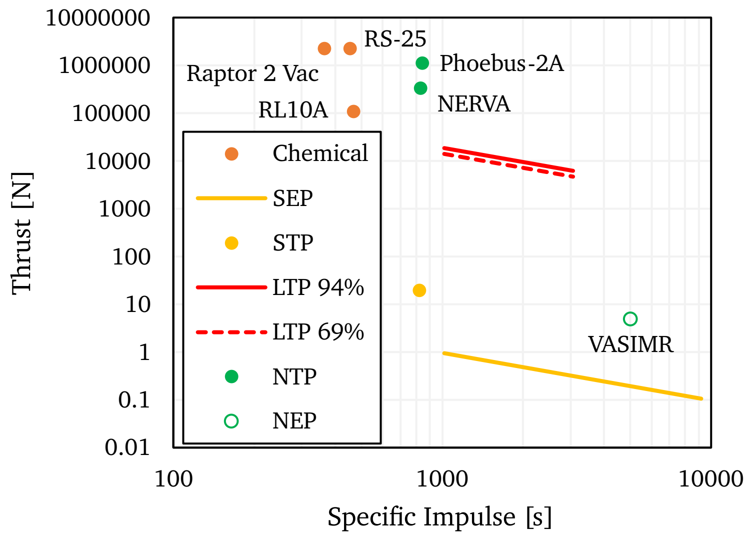

Figure 3.4: Comparison of several types of propulsion systems

- The recently flown NEXT-C [45] is used to represent the current state-of-the-art in terms of solar-electric propulsion (SEP)
- Solar-Thermal Propulsion, as discussed by Woodcock [46]
- Laser-Thermal Propulsion, as discussed by Duplay *et al.* [6], combined with loss estimates from Shoji and Larson [30]

Note that while Figure 3.4 provides an idea of how these systems compare, many other relevant parameters should be considered for a comprehensive comparison. First, many of the options presented here are power-limited and can theoretically vary their specific impulse and thrust—this is reflected in the curves of LTP and SEP, and is also applicable to nuclear systems. Second, such power-limited propulsion systems should also be compared in terms of conversion efficiency from the input power to jet power, and specific mass α. For now, it can be seen that LTP occupies a niche of moderate thrust and high specific impulse that is not occupied by many competing systems. LEP, which is not featured in the plot, also occupies this niche along approximately the same curve as LTP, though at greater specific impulses, as discussed by Sheerin *et al.* [13].

If LEP occupies a similar niche as LTP in terms of thrust and exhaust velocity, another figure of merit should be used to compare the performance of both systems and select the most appropriate option for a given mission. As discussed by Stuhlinger [47] in 1967, a propulsion system's specific power—or its reciprocal, specific mass—is a driving determinant of its suitability for a given mission. By characterizing a mission by the duration of its thrust maneuver t_{m} and its associated Δv, one can place constraints on the propulsion system's specific mass and exhaust velocity, and optimize these parameters to maximize the payload mass ratio.For example, high Δv maneuvers occurring over a few minutes (e.g., launch) will favor thrust over specific impulse in order to deliver the required Δv quickly. Alternatively, if a maneuver is less time-constrained (e.g., sending a probe to the outer solar system), low-thrust, high specific impulse systems will generally provide a better payload mass ratio. In the case of comparing LEP to LTP, Duplay *et al.* [6] provide an illustrative example, showing that LTP's lower specific mass allows it to perform similar missions as

LEP with much shorter maneuver duration, thus requiring smaller and fewer laser arrays than its electric counterpart, as mentioned in Section 2.2. However, if maneuver duration is allowed to extend to days and months, LEP's higher specific impulse allows it to outperform LTP.

LTP's theoretical specific impulse has however yet to be measured in laboratory conditions. Although many experiments have been performed, experimental values for the specific impulse, tabulated in Table 3.1, are still far from the 2000 s to 3000 s thought to be achievable in the literature. This may be due to several reasons. Many experiments were done using inert gases such as argon or nitrogen, which are simpler to work with but provide a lower exhaust velocity due to their increased molar mass compared to hydrogen. Furthermore, hydrogen does not readily absorb the heat radiated by the plasma, likely necessitating particle seeding to reduce heat losses to the walls. This was not done in the experiments listed below, reducing the resulting specific impulse. Finally, relatively small area ratio nozzles were used in these experiments (15:1 for Black *et al.* [4] and 36:1 for Toyoda *et al.* [48]), further reducing thruster performance under vacuum conditions as a result of under-expanded exhaust.

Table 3.1: Values of specific impulses achieved experimentally

Study	Gas	Laser power [W]	Specific impulse [s]
Black *et al.* [4]	Argon	7000	92.8
—	Hydrogen	8200	334.5
Toyoda *et al.* [48]	Argon	2000	113.0
—	Nitrogen	2000	108.0

Chapter 4

Experimental Methods

Given that the objective of the thesis project following this literature review involves the testing of a laboratory-scale laser-thermal thruster prototype, a review of the relevant experimental methods for such experiments is necessary. An overview of past experiments on LSP will be given to identify common approaches and critical apparatus. A brief discussion of available laser systems will also be included, along with an overview of relevant measurement apparatus, with specific attention given to thrust stand designs, including those built at TU Delft for small thruster experiments.

4.1 LSP experiments

Although a discussion of some LSP experiments was given in Chapter 3, some will be briefly revisited to focus on their experimental methods. Most experiments, including the very first LSP by Generalov *et al.* [34], used CO_2 lasers operating 10.6 µm. However, the optical setups, diagnostics, working gases, and configurations vary greatly. Facilities from three research groups will be discussed in particular, for their significant published research output and relevance to propulsion applications: the facility at the University of Illinois (late 1980s), at the University of Tennessee (late 1980s), and at the University of Tokyo, which published an LSP paper as recently as 2019.

University of Illinois Urbana-Champaign This facility (depicted in Figure 4.1a) was operated principally by Krier and Mazumder and was designed to characterize the energy conversion ability of LSPs, using Argon as a working fluid in most cases. According to Schwartz *et al.* [50], the LSP was sustained using a CO_2 laser with a maximum power of 10 kW, though it was never operated beyond 9 kW, with another 2 kW lost through the optics. The beam was focused into the absorption chamber with an elaborate set of reflective optics, that allowed the maintenance of dual-plasma geometry. Initiation of the plasma was achieved using a tungsten rod as a solid target, which was removed directly after plasma initiation using a solenoid actuator. The working fluid was Argon for most experiments, at 1.0 atm to 2.7 atm of gauge pressure. The absorption chamber design features devices to straighten and accelerate gas flow upstream of the LSP, facilitating the maintenance of a plasma at high flow rates. These design features include a flow straightener as the gas inlet section, and a converging quartz nozzle, which enabled the acceleration of the chamber flow without the need to manufacture a narrower thrust chamber, as the facility was initially designed for low flow speeds (< 2 m/s) (Krier *et al.* [49]). Most of their

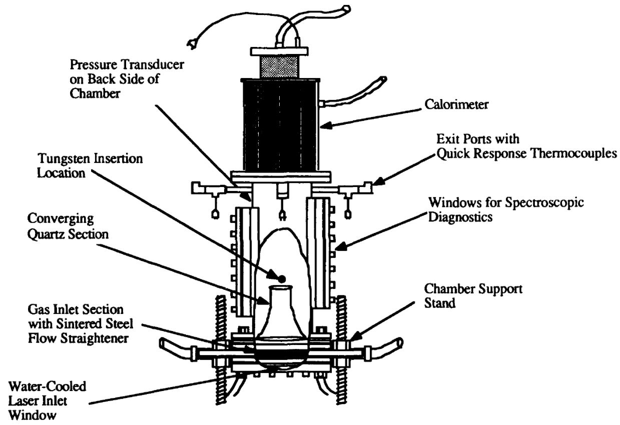

(a) UIUC LSP experiment [49].

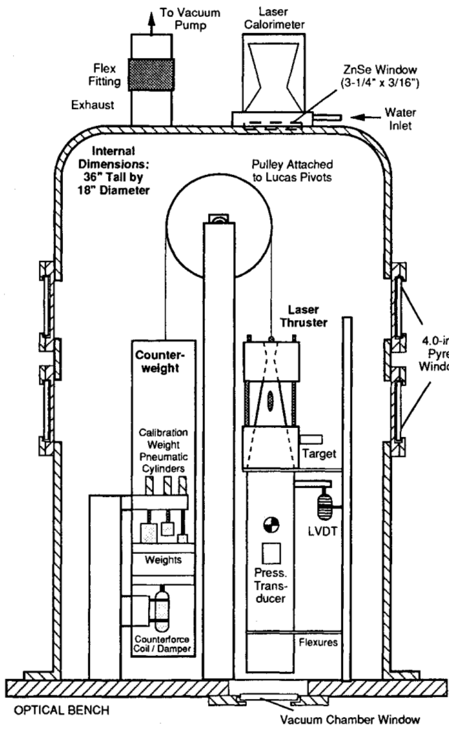

(b) Thruster and thrust stand [4]

Figure 4.1: UIUC experimental configurations

experiments revolved around laser absorption and thermal radiation, with little interest in thrust characteristics, so the heated gas exhaust was simply feed through exit ports. Nevertheless, experiments at this facility eventually led to the design and operation of a 10-kW-class thruster by Black *et al.* [4], with a 15:1 expansion ratio nozzle, achieving a specific impulse of up to 350 s, thermal efficiencies near 40 %, and thrust exceeding 3 N using hydrogen propellant. Their thrust stand, like their LSP experiments, used a vertical configuration with a pulley and counterweight. The entire stand was encapsulated in a vacuum chamber. Thrust measurements were performed using a combination of a linear variable differential transformer, which senses the displacement of the thruster, and a "counterforce coil", which uses the detected displacement and attempts to counteract it. The current supplied to the coil can be correlated to the thrust force F_T. This force could then be used with a measured mass flow rate $\dot{m}$ to compute specific impulse I_{sp} with Equation 4.1, which follows from thermal rocket theory (Zandbergen [14]).

$$I_{sp} = \frac{F_T}{\dot{m} g_0} \tag{4.1}$$

University of Tennessee Space Institute The UTSI experiments were run using a 1.5-kW-class CO_2 laser. This facility is contemporary of the one at UIUC and shares similar design features, such as the vertical configuration and the converging gas inlet. Both facilities' absorption chambers are made in large parts out of quartz walls to allow for spectroscopic measurements. In experiments performed by Keefer *et al.* [51], Argon was used as the working fluid, at pressures ranging from 1.3 atm to 2.3 atm, and laser powers as low as 360 W. A significant feature of their facility is the presence of specialized laser beam dump integrated within the converging exit nozzle.

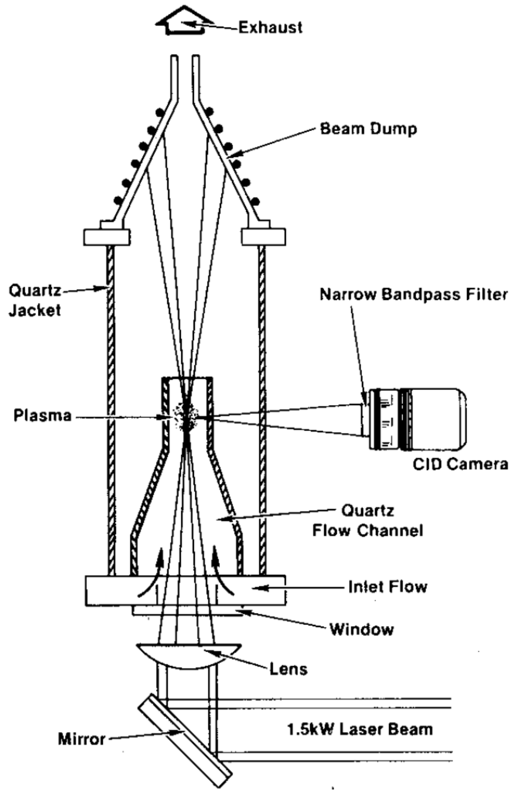

Figure 4.2: UTSI LSP apparatus [51]

University of Tokyo The most recent LSP experiments have been performed at the University of Tokyo, studying not only the characteristics of LSP (Inoue *et al.* [52]), but also investigating its propulsion performance, and its applications for replicating atmospheric re-entry conditions in wind tunnels (Matsui *et al.* [53]). The japanese facility (illustrated in Figure 4.3a) took a different approach to that of UIUC and UTSI, opting for a horizontally configured thrust stand. Instead of running the entire thruster within a vacuum chamber, the nozzle was connected to a separate vacuum tank by means of an expansion joint. This allowed the thruster to exhaust to vacuum conditions with reduced complexity, and without preventing the thruster from applying a force to the load cell. The Tokyo research group performed experiments using a variety of working gases, laser powers, and plasma initiation methods. Matsui *et al.* [54] even performed experiments with disk, fiber, and diode lasers, a major change from the traditional use of CO_2 lasers.

The japanese LSP chambers generally follow a similar design as those of UIUC and UTSI, i.e., a cylindrical section followed by a converging-diverging nozzle. However, they do not feature some of the additional flow control devices seen in the other facilities, such as the converging gas inlet channel. Instead, it appears many of their LSPs are maintained just downstream of the cylindrical section, which then allows the flow to naturally develop before it reaches the plasma. The gas inlet is also placed close to the nozzle, forcing the gas to flow between the internal and external walls of the thruster before entering the main chamber near the laser window, acting as a regenerative cooling system. The thruster also features a two-stage converging nozzle, with a subchamber in which the LSP is moved to after initiation, resulting in improved thrust levels (Toyoda *et al.* [48]). This is likely due to the improved absorption ability of LSP at higher flow speeds observed by Welle *et al.* [35].

The thrust measurement method used by Toyoda *et al.* [48] is also considerably simpler than the implementation used by Black *et al.* [4]. The thruster is mounted on low-friction linear rails and placed in contact with a load-cell. Weights on a pulley are used to balance the initial loads on the thruster. When operating the thruster to vacuum exhaust, the spring constant of the expansion joint was taken into account and compensated for. Furthermore, the motor was first run as a cold-gas thruster, using this initial thrust level as a reference to quantify the effect of the LSP.

Two methods of plasma initiation were used throughout their experiments. Early thruster studies used a tungsten rod in the same manner as Schwartz *et al.* [50] at UIUC. A later study by Matsui *et al.* [54] used an arc discharge at the laser focus point, seen in Figure 4.3b. This solid-state method of plasma initiation is attractive for its mechanical simplicity and its ability to quickly react to control inputs.

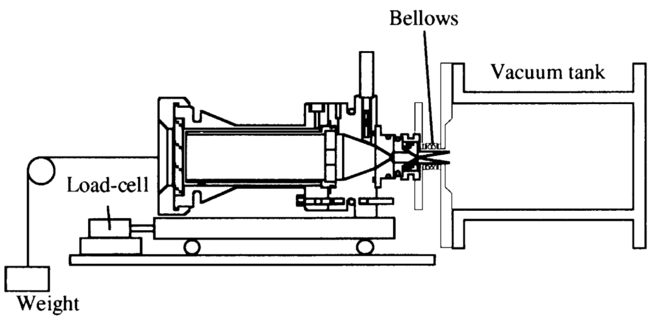

(a) Thrust measurement [48]

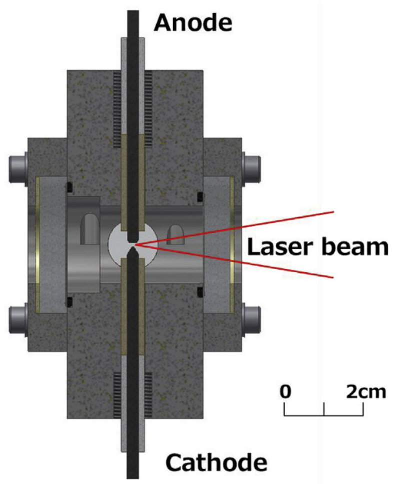

(b) LSP initiation through arc discharge [54]

Figure 4.3: University of Tokyo LSP apparatus

4.2 Laser system

The laser system available for LTP experiments at McGill University is an IPG Photonics YLR-300/3000-QCW-MM-AC Ytterbium fiber laser (referred to as “the laser system” from now on). Its specifications (available in Appendix A) will be briefly discussed, as they will place constraints on the experimental parameter space. The laser system is a 300 W continuous-wave fiber laser operating at a wavelength of 1070 nm, which is representative of the type of laser considered for DEP arrays, as discussed in Section 2.3. In addition to CW mode, the system can also operate in a so-called *quasi*-continuous-wave (QCW) mode, delivering 10 ms pulses at 3 kW. While this may seem short, laser pulse durations are typically expressed in femto- or nanoseconds, and millisecond-long pulses can often be considered in the continuous-wave regime—such as damage threshold comparisons [55]—hence the QCW designation.

Although LSP experiments have been successfully performed at the 300 W power level, the ability to apply laser intensities an order of magnitude greater is desirable to facilitate LSP maintenance, even for a limited duration. However, it is unlikely that such a short pulse will allow a complete thrust measurement system to reach steady-state, so the dynamic response of the apparatus will need to be considered for pulsed thrust measurements.

4.3 Measurement

Studying the performance of LTP will require the use of a thrust stand. For a thesis project at McGill University, a stand will have to be designed and constructed from scratch. Therefore, several existing designs used in past theses at TU Delft, past LSP experiments, and other rocketry projects will be reviewed in this section. A discussion of thrust measurement methodology is also included.

4.3.1 Thrust stands

University of Tokyo The experiments performed by Toyoda *et al.* [48] are a good candidate for reproduction thanks to the simplicity of their apparatus and comparable laser power used. Unfortunately, little detail is given on the design of their thrust stand. Figure 4.3a and Hosoda *et al.* [56] imply that the thruster was allowed to roll freely along horizontal rails, providing a “force-free condition” in the thrust direction. One thing to note is that they performed their experiments in continuous-wave mode, allowing the use of a relatively simple thrust measurement system: upon thruster ignition, enough time is given for the thrust stand to reach steady-state conditions, so oscillations in the thrust measurement can be ignored and the motor thrust can be determined in a straightforward manner. However, as alluded to in Section 4.2, this may not be feasible for thrust experiments performed in pulsed mode.

Delft University of Technology Delft’s Aerospace Engineering faculty has an extensive experience with thruster studies, through the work of numerous Spaceflight MSc. students and the Delft Aerospace Rocket Engineering (DARE) student team. Past MSc. studies are of particular interest as they typically considered low-thrust systems, of comparable or lower thrust levels to those of laboratory-scale LTP thrusters.

Takken [7] provides an overview of several thrust benches developed at TU Delft for small thruster experiments, as he considered repurposing them for testing of his solar-thermal thruster. He first discusses the AE-TB-1.1 thrust bench designed by Federica Valente in 2007, a pendulum design depicted in Figure 4.4a. Its noise levels were deemed too large to perform the low-thrust (0.1 N to 0.3 N) experiments considered with an STP thruster. Takken then considered the AE-TB-50m thrust bench (Figure Figure 4.4b) originally designed by Stef Janssens in 2009, then rebuilt by Krusharev [57] in 2015, rated for a maximum thrust of 50 mN. The TB-50m adopts a pivoting design, where the thrust force is transmitted to a load cell through a lever, instead of linearly along rails. This has a few advantages: selecting appropriate distances between the pivot, load cell, and thruster can allow the thruster to apply greater force on both the pivot and load cell through mechanical advantage. This can serve as a way to amplify the thrust signal, and overcome frictional forces in the pivot. This configuration also allows to offset much of the apparatus away from the laser beam path, reducing the likelihood of damaging it or causing reflections.

Jansen [58] also provides a similar discussion of thrust benches developed at TU Delft. Their thesis eventually focused on the AE-TB-5m thrust bench, a pendulum design rated for thrusts of up to 5 mN, depicted in Figure 4.4c. This shares many of the advantages listed for the TB-50m stand. However, this pendulum is designed to swing by a measurable angle. While this angle could theoretically be kept small, this method may not be suitable for an LTP engine, as the LSP may be sensitive to laser alignment with respect to the flow in the chamber.

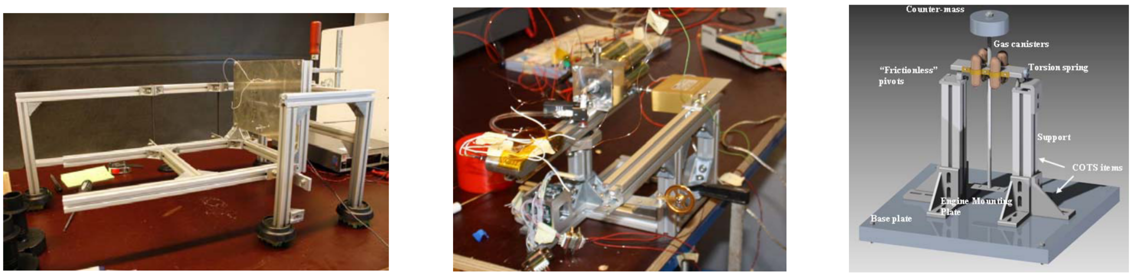

(a) AE-TB-1.1 (b) AE-TB-50m (c) AE-TB-5m

Figure 4.4: Various TU Delft micro thruster test benches, taken from Zandbergen *et al.* [59]

4.3.2 Thrust measurement

Thrust will be the primary variable measured to quantify thruster performance, so special attention must be given to its measurement. The likely operation of the LTP thruster in pulsed mode makes this non-trivial, as waiting for steady-state thrust conditions is likely not possible. Oscillations will likely not have dampened out before the end of the pulse, so detailed processing of the collected data will be necessary to determine the engine thrust, using the equation of motion of a spring-mass-damper system, as discussed by Zandbergen *et al.* [59]. The general form of this equation is as follows, where x, $\dot{x}$, and $\ddot{x}$ are the displacement, velocity, and acceleration of the mass m on a system oscillating due to the time-varying force $F(t)$.

$$m\ddot{x} + c_\mathrm{d}\dot{x} + kx = F(t) \tag{4.2}$$

The damping factor c_d and stiffness k are characteristics of the thrust bench which must be predicted and/or derived experimentally using the equations for the damped frequency of the system ω_d and the damping ratio ζ, which can be measured with a known impulsive force.

$$\omega_\mathrm{d} = \omega_\mathrm{n}\sqrt{1-\zeta^2} \tag{4.3}$$

$$\zeta = \frac{c_\mathrm{d}}{2m\omega_\mathrm{n}} \tag{4.4}$$

$$\omega_\mathrm{n} = \sqrt{\frac{k}{m}} \tag{4.5}$$

Once these parameters have been determined, the reverse procedure can be performed to determine the magnitude of an impulsive force F, knowing that the displacement response of the system will be of the following form (Zandbergen *et al.* [59]):

$$x(t) = \frac{F}{m\omega_\mathrm{d}}\mathrm{e}^{-\zeta\omega_\mathrm{n}t}\sin\left(\omega_\mathrm{d}t\right) \tag{4.6}$$

The value of the impulsive thrust can thus be determined based from the oscillatory displacement readings of the thrust stand. While a load cell may appear to be a straightforward method of determining thrust, particularly for CW laser operation, a displacement sensor or accelerometer may be more appropriate for pulsed operation, to take advantage of the vibration characteristics of the system.

Chapter 5

Conclusion

Maintaining a human presence beyond Earth orbit and enabling the human exploration of the outer solar system calls for more powerful and efficient power and propulsion systems. Laser-thermal propulsion offers high specific-impulse and high thrust, a propulsion niche that fulfills rapid interplanetary transit needs but is not occupied by any propulsion concept in current use. This literature review considered the current body of literature relevant to laser-thermal propulsion, from the parent field of directed-energy propulsion to the implementation of various low-thrust test stands for eventual experiments as part of a Master's thesis project.

The field of directed-energy propulsion, the general concept of remotely powering spacecraft using lasers or masers for power transmission, was reviewed, with a discussion of relevant laser physics and the various proposed implementations of DEP, including their strengths and weaknesses. While the concept is several decades old, the recent developments in fiber laser optics are highlighted as an enabling technology for the near-term realization of DEP, by means of large phase-locked laser arrays operating at a wavelength of 1064 nm. It was found that the same technology used by astronomers to correct for atmospheric distortion can be used in the reverse direction to maintain diffraction-limited laser spots in outer space. The architecture of DEP laser arrays is sound and does not exhibit any fundamental technical flaws.

Specific attention was then given to laser-plasma propulsion, an LTP concept where the laser power is directly coupled to a propellant via a laser-sustained plasma, allowing direct heat deposition in the propellant which can then be expanded through a conventional rocket nozzle. LSP has been studied theoretically and experimentally since the 1970s, and its maintenance has been achieved under a variety of conditions, in several working gases. The high temperatures attained in the LSP theoretically allow for much greater specific impulses to be delivered than in chemical rocket thrusters or even nuclear-thermal systems. LSP is thought to be capable of achieving nearly complete laser absorption under some conditions, and high thermal efficiencies could be achieved through particle seeding, suggesting that high overall efficiencies can be attained in a well-designed laser-thermal thruster. Such a propulsion system would readily compete with nuclear-thermal or laser-electric propulsion systems for rapid, high-mass and high Δv missions powered by a single laser array. Nevertheless, the current state of experimental LTP thruster is still far from achieving the specific impulses predicted by theory, so there is an opportunity for further work in this area.

Finally, the experimental methods used in past LSP and small thruster experiments were reviewed, in order to replicate them for a future LTP experiment at McGill University. In the interest of determining the thrust characteristics of an LTP thruster, prototype engine and thrust stand designs were reviewed, both from LSP literature and past Master's projects at TU Delft. Several thrust measurement methods were reviewed, including the use of the thrust stand's dynamic response to determine pulsed thrust magnitude. This method is deemed highly relevant for a future experiment at McGill University, as the available laser system is only able to deliver 3 kW of power for 10 ms.

The body of literature on directed-energy propulsion architectures, mission designs, laser-sustained plasma, and laser-thermal propulsion suggest the concept is feasible and would unlock a class of missions of high interest for piloted interplanetary spaceflight. However, although LSP continues to be studied for various applications, CW laser-plasma propulsion experiments remain scarce, and the performance achieved is still far from theoretical predictions. In addition, thrust experiments have yet to be performed using 1 μm fiber lasers, and it is known that the laser wavelength affects the absorption ability of LSP via inverse-brehmsstrahlung. The availability of fiber lasers that can readily be assembled in the large arrays needed for DEP provide a strong interest in LTP, and a significant research gap exists in both the feasibility of LTP with 1 μm lasers and in improving its specific impulse up to its theoretical limits.

References

[1] D. L. Nored, "Application of high power lasers to space power and propulsion," in *2d NASA Conf. on Laser Energy Conversion*, National Aeronautics and Space Administration, Jan. 1, 1976. [Online]. Available: https://ntrs.nasa.gov/citations/19760014427.

[2] J. T. Kare, "Laser Launch—The Second Wave," in *AIP Conference Proceedings*, vol. 664, Huntsville, Alabama (USA): AIP, 2003, pp. 22–36. DOI: 10.1063/1.1582093. [Online]. Available: http://aip.scitation.org/doi/abs/10.1063/1.1582093.

[3] L. Myrabo, "World record flights of beam-riding rocket lightcraft - Demonstration of "disruptive" propulsion technology," in *37th Joint Propulsion Conference and Exhibit*, Salt Lake City,UT,U.S.A.: American Institute of Aeronautics and Astronautics, Jul. 8, 2001. DOI: 10.2514/6.2001-3798. [Online]. Available: https://arc.aiaa.org/doi/10.2514/6.2001-3798.

[4] J. Black, H. Krier, and R. J. Glumb, "Laser Propulsion 10-kW Thruster Test Program results," *Journal of Propulsion and Power*, vol. 11, no. 6, pp. 1307–1316, Nov. 1995, ISSN: 0748-4658, 1533-3876. DOI: 10.2514/3.23973. [Online]. Available: https://arc.aiaa.org/doi/10.2514/3.23973.

[5] P. Lubin, *A Roadmap to Interstellar Flight*, Comment: 60 pages, 30 figures. Submitted to JBIS April 2015, Jan. 21, 2022. DOI: 10.48550/arXiv.1604.01356. arXiv: 1604.01356 [astro-ph, physics:physics]. [Online]. Available: http://arxiv.org/abs/1604.01356.

[6] E. Duplay, Z. F. Bao, S. Rodriguez Rosero, A. Sinha, and A. Higgins, "Design of a rapid transit to Mars mission using laser-thermal propulsion," *Acta Astronautica*, vol. 192, pp. 143–156, Mar. 1, 2022, ISSN: 0094-5765. DOI: 10.1016/j.actaastro.2021.11.032. [Online]. Available: https://www.sciencedirect.com/science/article/pii/S0094576521006305.

[7] A.-J. Takken, "Development of a high-temperature Solar Thermal Propulsion engine," M.S. thesis, Delft University of Technology, Delft, 2021. [Online]. Available: https://repository.tudelft.nl/islandora/object/uuid%3Ae6cc6c72-bcfb-4927-a0bf-d935a6ba32f8.

[8] J. Hecht, *Understanding Lasers: An Entry Level Guide*, 4th ed. Hoboken: John Wiley & Sons, Inc., 2019, ISBN: 978-1-119-31064-8.

[9] M. G. R. Urbanczyk, "Solar Sails -A Realistic Propulsion for Spacecraft," Technical Memorandum NASA-TM-X-60560, Aug. 2, 1967. [Online]. Available: https://ntrs.nasa.gov/citations/19670030985.

[10] O. Mori *et al.*, "First Solar Power Sail Demonstration by IKAROS," *Transactions of the Japanese Society for Artificial Intelligence*, vol. 8, To_4, Jan. 1, 2011, ISSN: 1346-0714. [Online]. Available: https://ui.adsabs.harvard.edu/abs/2011TJSAI...8To425M.

[11] P. Lubin and W. Hettel, "The Path to Interstellar Flight," Apr. 10, 2020. DOI: 10.5281/ZENODO.3747263. [Online]. Available: https://zenodo.org/record/3747263.

[12] J. R. Brophy *et al.*, "Directed-energy propulsion architecture for deep-space missions with characteristic velocities of order 100 km/s," in *36th International Electric Propulsion Conference*, Pasadena, CA: Jet Propulsion Laboratory, NASA, Sep. 2019. [Online]. Available: http://hdl.handle.net/2014/51719.

[13] T. F. Sheerin, E. Petro, K. Winters, P. Lozano, and P. Lubin, "Fast Solar System transportation with electric propulsion powered by directed energy," *Acta Astronautica*, vol. 179, pp. 78–87, Feb. 1, 2021, ISSN: 0094-5765. DOI: 10.1016/j.actaastro.2020.09.016. [Online]. Available: https://www.sciencedirect.com/science/article/pii/S0094576520305567.

[14] B. T. C. Zandbergen, *AE4-S01 Thermal Rocket Propulsion*, 2.08. TU Delft, Aug. 20, 2020.

[15] J. F. Geisz *et al.*, "Six-junction III–V solar cells with 47.1% conversion efficiency under 143 Suns concentration," *Nature Energy*, vol. 5, no. 4, pp. 326–335, 4 Apr. 2020, ISSN: 2058-7546. DOI: 10.1038/s41560-020-0598-5. [Online]. Available: http://www.nature.com/articles/s41560-020-0598-5.

[16] H. Helmers *et al.*, "68.9% Efficient GaAs-Based Photonic Power Conversion Enabled by Photon Recycling and Optical Resonance," *physica status solidi (RRL) – Rapid Research Letters*, vol. 15, no. 7, p. 2 100 113, 2021, ISSN: 1862-6270. DOI: 10.1002/pssr.202100113. [Online]. Available: http://onlinelibrary.wiley.com/doi/abs/10.1002/pssr.202100113.

[17] A. Kantrowitz, "The Relevance of Space," *Bulletin of the Atomic Scientists*, vol. 27, no. 4, pp. 32–33, Apr. 1, 1971, ISSN: 0096-3402. DOI: 10.1080/00963402.1971.11455353. [Online]. Available: https://doi.org/10.1080/00963402.1971.11455353.

[18] K. Mori, "Beamed Launch Propulsion," in *Propulsion Systems*, Rijeka: IntechOpen, Oct. 2019, ISBN: 978-1-83962-280-9. [Online]. Available: http://dx.doi.org/10.5772/intechopen.82236.

[19] H.-A. Eckel and W. Schall, "Laser Propulsion Systems," in *Advanced Propulsion Systems and Technologies, Today to 2020*, American Institute of Aeronautics and Astronautics, pp. 357–406, ISBN: 978-1-56347-929-8. DOI: 10.2514/5.9781600866937.0357.0406. [Online]. Available: https://arc.aiaa.org/doi/abs/10.2514/5.9781600866937.0357.0406.

[20] L. N. Myrabo, "Power-Beaming Technology for Laser Propulsion," in *Orbit-Raising and Maneuvering Propulsion: Research Status and Needs*, New York: American Institute of Aeronautics and Astronautics, Jan. 1, 1984, ISBN: 978-0-915928-82-8 978-1-60086-563-3. DOI: 10.2514/4.865633. [Online]. Available: https://arc.aiaa.org/doi/book/10.2514/4.865633.

[21] E. Meloney, L. Myrabo, H. Nagamatsu, and R. Bracken, "Experimental investigation of a 2-D MHD slipstream accelerator - Progress report,"

in *37th Joint Propulsion Conference and Exhibit*, Salt Lake City,UT,U.S.A.: American Institute of Aeronautics and Astronautics, Jul. 8, 2001. DOI: `10.2514/6.2001-3799`. [Online]. Available: `https://arc.aiaa.org/doi/10.2514/6.2001-3799`.

[22] J. T. Kare, "Laser-powered heat exchanger rocket for ground-to-orbit launch," *Journal of Propulsion and Power*, vol. 11, no. 3, pp. 535–543, May 1995, ISSN: 0748-4658, 1533-3876. DOI: `10.2514/3.23875`. [Online]. Available: `https://arc.aiaa.org/doi/10.2514/3.23875`.

[23] D. Keefer, R. Elkins, C. Peters, and L. W. Jones, "Laser-Thermal Propulsion," in *Orbit-Raising and Maneuvering Propulsion: Research Status and Needs*, New York: American Institute of Aeronautics and Astronautics, Jan. 1, 1984, ISBN: 978-0-915928-82-8 978-1-60086-563-3. DOI: `10.2514/4.865633`. [Online]. Available: `https://arc.aiaa.org/doi/book/10.2514/4.865633`.

[24] Gemini Observatory. "The Sites," Gemini Observatory. (Apr. 3, 2020), [Online]. Available: `https://www.gemini.edu/observing/telescopes-and-sites/sites#0.9-2.7um`.

[25] S. P. Worden, W. A. Green, J. Schalkwyk, K. Parkin, and R. Q. Fugate, "Progress on the Starshot laser propulsion system," *Applied Optics*, vol. 60, no. 31, H20–H23, Nov. 1, 2021, ISSN: 2155-3165. DOI: `10.1364/AO.435858`. [Online]. Available: `https://opg.optica.org/ao/abstract.cfm?uri=ao-60-31-H20`.

[26] W. Hettel *et al.*, "Beam propagation simulation of phased laser arrays with atmospheric perturbations," *Applied Optics*, vol. 60, no. 17, pp. 5117–5123, Jun. 10, 2021, ISSN: 2155-3165. DOI: `10.1364/AO.422337`. [Online]. Available: `https://www.osapublishing.org/ao/abstract.cfm?uri=ao-60-17-5117`.

[27] H. A. Arbit, S. D. Clapp, and C. K. Nagai, "Lithium-fluorine-hydrogen propellant investigation Final report," Contractor Report NASA-CR-72695, May 1, 1970. [Online]. Available: `https://ntrs.nasa.gov/citations/19700018655`.

[28] Aerojet Rocketdyne. "RL10 Engine," Aerojet Rocketdyne. (), [Online]. Available: `https://www.rocket.com/space/liquid-engines/rl10-engine`.

[29] H. P. Gerrish, "Solar Thermal Propulsion at MSFC," Feb. 3, 2016. [Online]. Available: `https://ntrs.nasa.gov/citations/20160003173`.

[30] J. Shoji and V. Larson, "Performance and heat transfer characteristics of the laser-heated rocket - A future space transportation system," in *12th International Electric Propulsion Conference*, ser. International Electric Propulsion Conference, American Institute of Aeronautics and Astronautics, Nov. 14, 1976. DOI: `10.2514/6.1976-1044`. [Online]. Available: `https://arc.aiaa.org/doi/10.2514/6.1976-1044`.

[31] D. Keefer, "Laser-Sustained Plasmas," in *Laser Induced Plasmas and Applications*, New York: MARCEL DEKKER INC., 1989, ISBN: 0-8247-8078-7.

[32] R. J. Glumb and H. Krier, "Concepts and status of laser-supported rocket propulsion," *Journal of Spacecraft and Rockets*, vol. 21, no. 1, pp. 70–79, Jan. 1, 1984, ISSN: 0022-4650. DOI: `10.2514/3.8610`. [Online]. Available: `https://arc.aiaa.org/doi/10.2514/3.8610`.

[33] Y. P. Raizer, "SUBSONIC PROPAGATION OF A LIGHT SPARK AND THRESHOLD CONDITIONS FOR MAINTENANCE OF A PLASMA BY RADIATION.," *Soviet Physics Journal of Experimental and Theoretical Physics*, vol. 31, no. 6, Dec. 1970. [Online]. Available: `https://www.osti.gov/biblio/4116864`.

[34] N. Generalov, V. Zimakov, G. Kozlov, V. Masyukov, and Y. P. Raizer, "Continuous optical discharge," *Soviet Journal of Experimental and Theoretical Physics Letters*, vol. 11, pp. 302–304, 1970.

[35] R. Welle, D. Keefer, and C. Peters, "Energy conversion efficiency in high-flow laser-sustained argon plasmas," in *AIAA/ASME 4th Fluid Mechanics, Plasma Dynamics and Lasers Conference*, Atlanta, May 1986. [Online]. Available: `https://ui.adsabs.harvard.edu/abs/1986aiaa.confT....K`.

[36] M. C. Fowler and D. C. Smith, "Ignition and maintenance of subsonic plasma waves in atmospheric pressure air by cw CO2 laser radiation and their effect on laser beam propagation," *Journal of Applied Physics*, vol. 46, no. 1, pp. 138–150, Jan. 1975, ISSN: 0021-8979. DOI: `10.1063/1.322197`. [Online]. Available: `https://aip.scitation.org/doi/10.1063/1.322197`.

[37] S.-M. Jeng and D. Keefer, "Numerical study of laser-sustained hydrogen plasmas in a forced convective flow," in *22nd Joint Propulsion Conference*, ser. Joint Propulsion Conferences, American Institute of Aeronautics and Astronautics, Jun. 16, 1986. DOI: `10.2514/6.1986-1524`.

[38] J. H. Batteh and D. R. Keefer, "Two dimensional generalization of Raizer's analysis for the subsonic propagation of laser sparks," *IEEE Trans. Plasma Sci., v. PS-2, no. 3, pp. 122-129*, Sep. 1, 1974. DOI: `10.1109/TPS.1974.4316825`. [Online]. Available: `https://www.osti.gov/biblio/4232630`.

[39] C. D. Moody, "Maintenance of a gas breakdown in argon using 10.6-µ cw radiation," *Journal of Applied Physics*, vol. 46, no. 6, pp. 2475–2482, Jun. 1975, ISSN: 0021-8979, 1089-7550. DOI: `10.1063/1.322232`. [Online]. Available: `http://aip.scitation.org/doi/10.1063/1.322232`.

[40] H. Krier, J. Mazumder, T. Rockstroh, T. Bender, and R. Glumb, "Continuous wave laser gas heating by sustained plasmas in flowing argon," *AIAA Journal*, vol. 24, no. 10, pp. 1656–1662, Oct. 1986, ISSN: 0001-1452. DOI: `10.2514/3.9497`. [Online]. Available: `https://arc.aiaa.org/doi/10.2514/3.9497`.

[41] M. V. Gerasimenko, G. I. Kozlov, and V. A. Kuznetsov, "Laser plasmatron," *Soviet Journal of Quantum Electronics*, vol. 13, no. 4, p. 438, Apr. 30, 1983, ISSN: 0049-1748. DOI: `10.1070/QE1983v013n04ABEH004189`. [Online]. Available: `https://iopscience-iop-org.tudelft.idm.oclc.org/article/10.1070/QE1983v013n04ABEH004189/meta`.

[42] Aerojet Rocketdyne. "RS-25 Engine," Aerojet Rocketdyne. (), [Online]. Available: `https://www.rocket.com/space/liquid-engines/rs-25-engine`.

[43] A. G. Belluscio. "SpaceX advances drive for Mars rocket via Raptor power," NASASpaceFlight.com. (Mar. 7, 2014), [Online]. Available: `https://www.nasaspaceflight.com/2014/03/spacex-advances-drive-mars-rocket-raptor-power/`.

[44] D. R. Koenig, "Experience Gained from the Space Nuclear Rocket Program (Rover)," Los Alamos National Laboratory, LA-10062-H, May 1986. [Online]. Available: http://nuke.fas.org/space/la-10062.pdf.

[45] Aerojet Rocketdyne, *NEXT-C NASA Evolutionary Xenon Thruster-Commercial*, Jan. 2022. [Online]. Available: https://www.rocket.com/sites/default/files/documents/NEXT-C_Data_sheet_01_2022_FINAL_DIGITAL.pdf.

[46] G. Woodcock, "Evaluation of Solar Thermal Propulsion for In-Space Propulsion Application," in *39th AIAA/ASME/SAE/ASEE Joint Propulsion Conference and Exhibit*, American Institute of Aeronautics and Astronautics. DOI: 10.2514/6.2003-5029. [Online]. Available: https://arc.aiaa.org/doi/abs/10.2514/6.2003-5029.

[47] E. Stuhlinger, "Electric space propulsion systems," *Space Science Reviews*, vol. 7, no. 5, pp. 795–847, Dec. 1, 1967, ISSN: 1572-9672. DOI: 10.1007/BF00542896.

[48] K. Toyoda, K. Komurasaki, and Y. Arakawa, "Thrust performance of a CW laser thruster in vacuum," *Vacuum*, 3rd International Symposium on Applied Plasma Science (ISAPS 01), vol. 65, no. 3, pp. 383–388, May 27, 2002, ISSN: 0042-207X. DOI: 10.1016/S0042-207X(01)00446-8. [Online]. Available: https://www.sciencedirect.com/science/article/pii/S0042207X01004468.

[49] H. Krier, J. Mazumder, D. K. Zerkle, A. Mertogul, and S. Schwartz, "Energy Conversion Measurements in Laser-Sustained Argon Plasmas for Application to Rocket Propulsion.," Department of Mechanical and Industrial Engineering University of Illinois at Urbana-Champaign, Technical Report UILU-ENG-88-4006, Apr. 15, 1988, p. 85. [Online]. Available: https://apps.dtic.mil/sti/citations/ADA194931.

[50] S. Schwartz *et al.*, "Laser-sustained gas plasmas for application to rocket propulsion," in *25th Joint Propulsion Conference*, Monterey,CA,U.S.A.: American Institute of Aeronautics and Astronautics, Jul. 12, 1989. DOI: 10.2514/6.1989-2631. [Online]. Available: https://arc.aiaa.org/doi/10.2514/6.1989-2631.

[51] D. Keefer, R. Welle, and C. Peters, "Power absorption in laser-sustained argon plasmas," *AIAA Journal*, vol. 24, no. 10, pp. 1663–1669, Oct. 1986, ISSN: 0001-1452. DOI: 10.2514/3.9498. [Online]. Available: https://arc.aiaa.org/doi/10.2514/3.9498.

[52] T. Inoue *et al.*, "Oscillation phenomenon of laser-sustained plasma in a CW laser propulsion," *Vacuum*, The 4th International Symposium on Applied Plasma Science, vol. 73, no. 3, pp. 433–438, Apr. 19, 2004, ISSN: 0042-207X. DOI: 10.1016/j.vacuum.2003.12.063. [Online]. Available: https://www.sciencedirect.com/science/article/pii/S0042207X03002926.

[53] M. Matsui, S. Yoneda, K. Komurasaki, Y. Yamagiwa, and Y. Arakawa, "Atomic-Oxygen-Flow Generation by Laser-Driven Plasma Wind Tunnel as Low-Earth-Orbit-Environment Simulator," *AIAA Journal*, vol. 52, no. 8, pp. 1806–1810, Aug. 2014, ISSN: 0001-1452, 1533-385X. DOI: 10.2514/1.J052991. [Online]. Available: https://arc.aiaa.org/doi/10.2514/1.J052991 (visited on 2022-12-08).

[54] M. Matsui, T. Ono, T. Kamei, and K. Mori, "Generating conditions of argon laser-sustained plasma by disk, fiber and diode lasers,"

Vacuum, vol. 167, pp. 490–494, Sep. 1, 2019, ISSN: 0042-207X. DOI: 10.1016/j.vacuum.2018.05.012. [Online]. Available: https://www.sciencedirect.com/science/article/pii/S0042207X18301751.

[55] Thorlabs. "Optical Coatings," Thorlabs, Inc. (), [Online]. Available: https://www.thorlabs.com/newgrouppage9.cfm?objectgroup_id=5840 (visited on 2022-10-30).

[56] S. Hosoda, K. Toyoda, K. Komurasaki, and Y. Arakawa, "Plasma diagnostics of laser-sustained plasma in a CW laser thruster," in *26th International Electric Propulsion Conference*, Kitakyushu, Oct. 1999. [Online]. Available: http://electricrocket.org/IEPC/9017.pdf.

[57] I. Krusharev, "Micro - Thruster Development: Propulsion System for the DelFFi Mission," 2015. [Online]. Available: https://repository.tudelft.nl/islandora/object/uuid%3Ae60e68fe-d1f6-458b-8a5a-d5036e32fb69.

[58] E. H. W. Jansen, "Improvement and validation of test stand performance for novel micropropulsion systems," M.S. thesis, Delft University of Technology, Delft, 2016. [Online]. Available: https://repository.tudelft.nl/islandora/object/uuid%3A28f0b7fa-1288-4e32-88fd-2e138745714a.

[59] B. T. C. Zandbergen, S. Janssens, F. Valente, D. Perez-Grande, and R. Koopmans, "Test facility development for testing of micro-thrusters at TU-Delft," *6th International Spacecraft Propulsion Conference, San Sebastian, Spain, 3-6 May 2010*, 2010. [Online]. Available: https://repository.tudelft.nl/islandora/object/uuid%3Aec41e926-e040-4483-bb24-2a742cce0b4a.

Appendix A

YLR-300/3000-MM-AC Datasheet

IPG PHOTONICS	**TEST RESULTS** **YTTERBIUM FIBER LASER** **Model YLR-300/3000-QCW-MM-AC** **S/N PLMP31901422**	Form: Revision: Spec: Page:	P69-00051 1 G22-29650 rev.4 1 of 6

This product is covered by the U.S. Pat. Nos. 5,422,897 and 5,774,484 and any foreign counterparts thereof, and other patents pending.

The information and the following charts provided below is the result of tests performed in controlled environments by IPG Photonics. These provided useful, but not warranted, information about the functions and performance of the product.

N	Characteristic	Symbol	Test Conditions	Min	Typ.	Max	Test Results	Unit
	Optical characteristics							
1.1	Operation Mode				Pulsed / CW		Pulsed / CW	
1.2	Maximum Average Power	$P_{average}$	Pulsed mode	300			307.9	W
		P_{CW}	CW mode	300			342.0	W
1.3	Maximum Peak Power	P_{peak}	Pulsed mode				3079.25	W
1.4	Duty Cycle	DC	Pulsed mode			50[1)]	Tested	%
1.5	Pulse Duration	τ	Pulsed mode	0.2		50[2)]	0.2-50	ms
1.6	Maximal Pulse Energy	E_{max}	Pulsed mode	30			30.8	J
1.7	Emission Wavelength	λ			1070		1069.6	nm
1.8	Emission Linewidth	$\Delta\lambda$	Pulsed mode maximum output power		5	6	1	nm
1.9	Long-term Power Instability		T = const maximum output power CW & Pulsed mode		± 0.5	± 1	± 0.5	%
	Optical output							
2.1	Output Fiber Termination				QBH-compatible connector		Tested	
2.2	Beam Quality	BPP[3)]	50µm core fiber pulsed mode	1		2	2	mm x mrad
	General characteristics							
3.1	Cooling Method				Forced Air			
	Electrical characteristics							
4.1	Operating Voltage, single phase				200-240 VAC, 50/60 Hz			VAC

[1)] Maximum duty cycle limit is inversely proportional to peak power: 10% for 3000W, 15% for 2000W, …, 50% for 600W and lower.
[2)] Maximum pulse duration limit is inversely proportional to peak power: 10ms for 3000W, 15ms for 2000W, …,50ms for 600W and lower.

3) Measurement tolerance for BPP is +/- 10%.

	TEST RESULTS YTTERBIUM FIBER LASER Model YLR-300/3000-QCW-MM-AC S/N PLMP31901422	Form: Revision: Spec: Page:	P69-00051 1 G22-29650 rev.4 2 of 6

N	Characteristic	Test Conditions	Test Results
	Laser interfaces		
5.1	Control	Analog	Tested
		RS-232	Tested
		Ethernet	Tested

Date: 29.10.2019

Tested by: Henry Thepsimoung

Approved by: Thomas Rogers

This document has been created automatically and is valid without a signature

	TEST RESULTS **YTTERBIUM FIBER LASER** **Model YLR-300/3000-QCW-MM-AC** **S/N PLMP31901422**	Form: Revision: Spec: Page:	P69-00051 1 G22-29650 rev.4 3 of 6

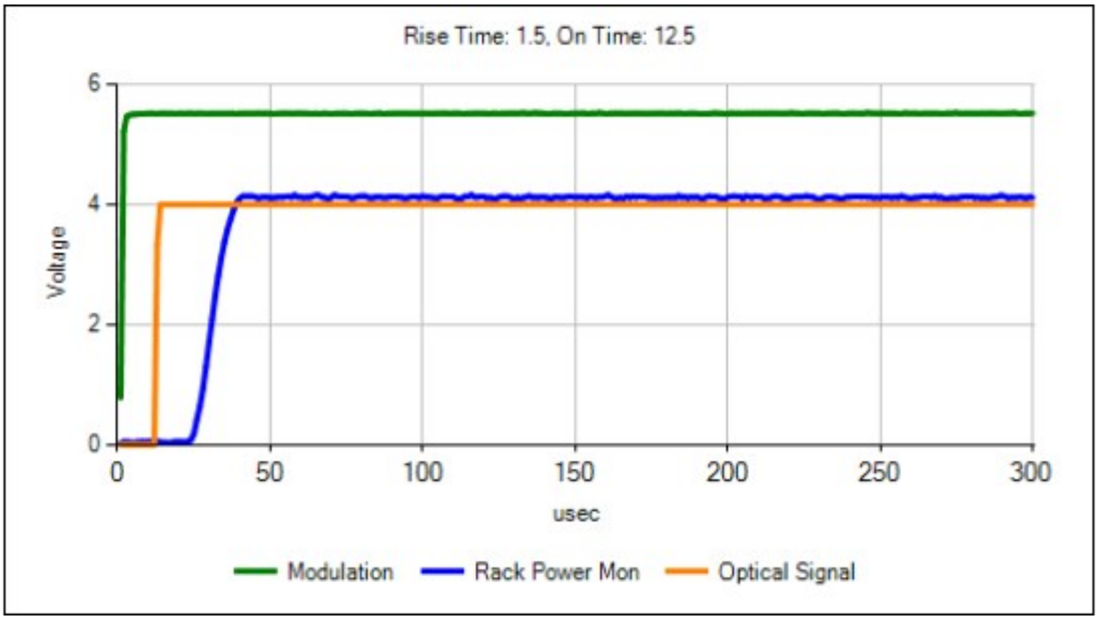

Fig. 1 Switching ON characteristic at nominal output power

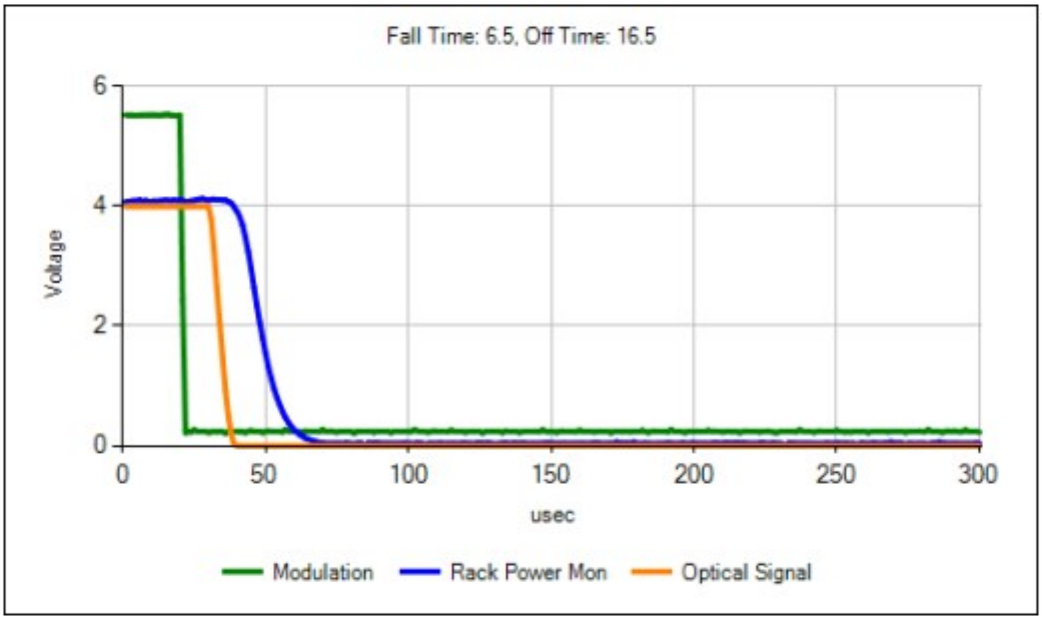

Fig. 2 Switching OFF characteristic at nominal output power

IPG PHOTONICS	**TEST RESULTS** **YTTERBIUM FIBER LASER** **Model YLR-300/3000-QCW-MM-AC** **S/N PLMP31901422**	Form: Revision: Spec: Page:	P69-00051 1 G22-29650 rev.4 4 of 6

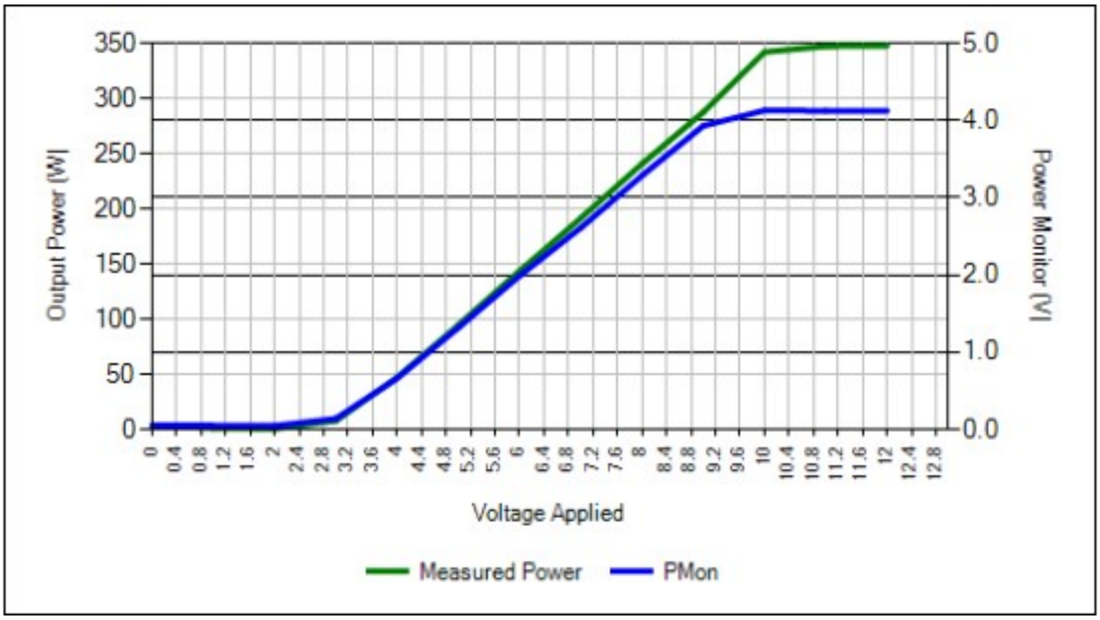

Fig. 3 CW Mode: Output Power vs.Analog Voltage

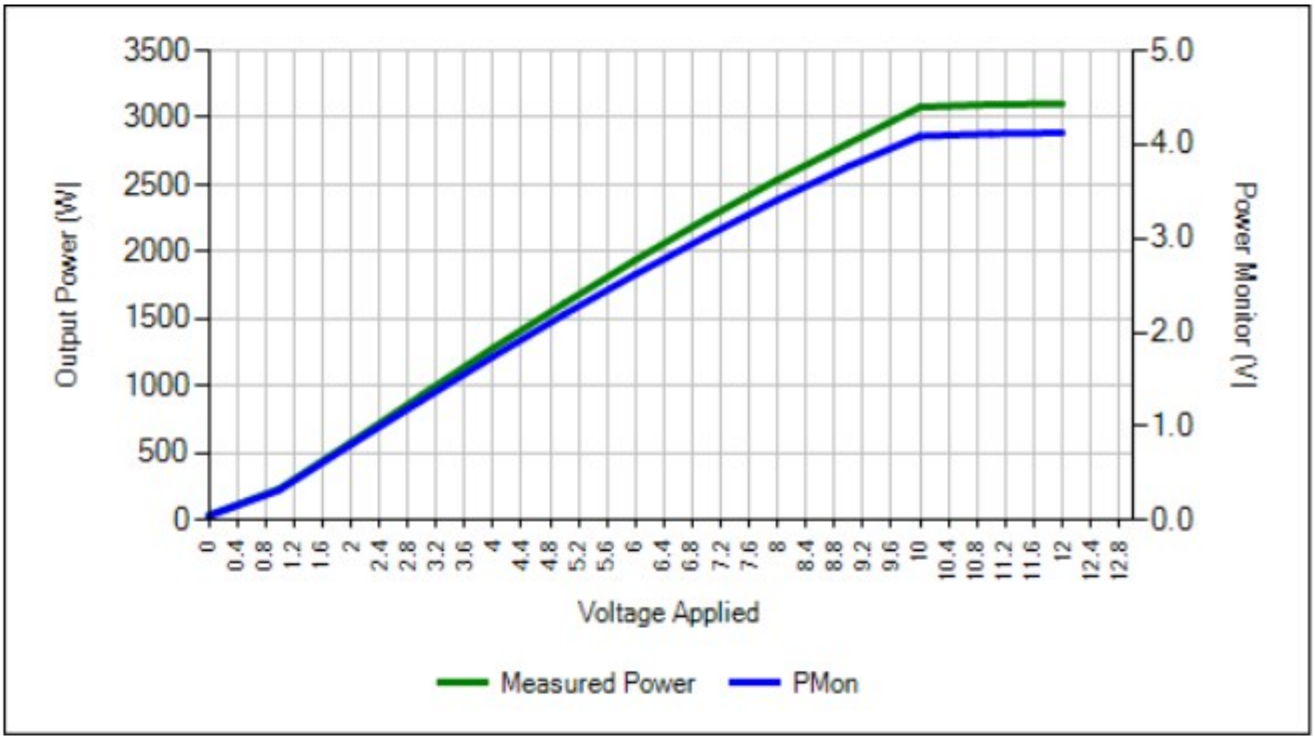

Fig. 4 Pulsed Mode: Peak Output vs. Analog Voltage at RR=10Hz, 10% Duty Cycle

	TEST RESULTS YTTERBIUM FIBER LASER Model YLR-300/3000-QCW-MM-AC S/N PLMP31901422	Form: Revision: Spec: Page:	P69-00051 1 G22-29650 rev.4 5 of 6

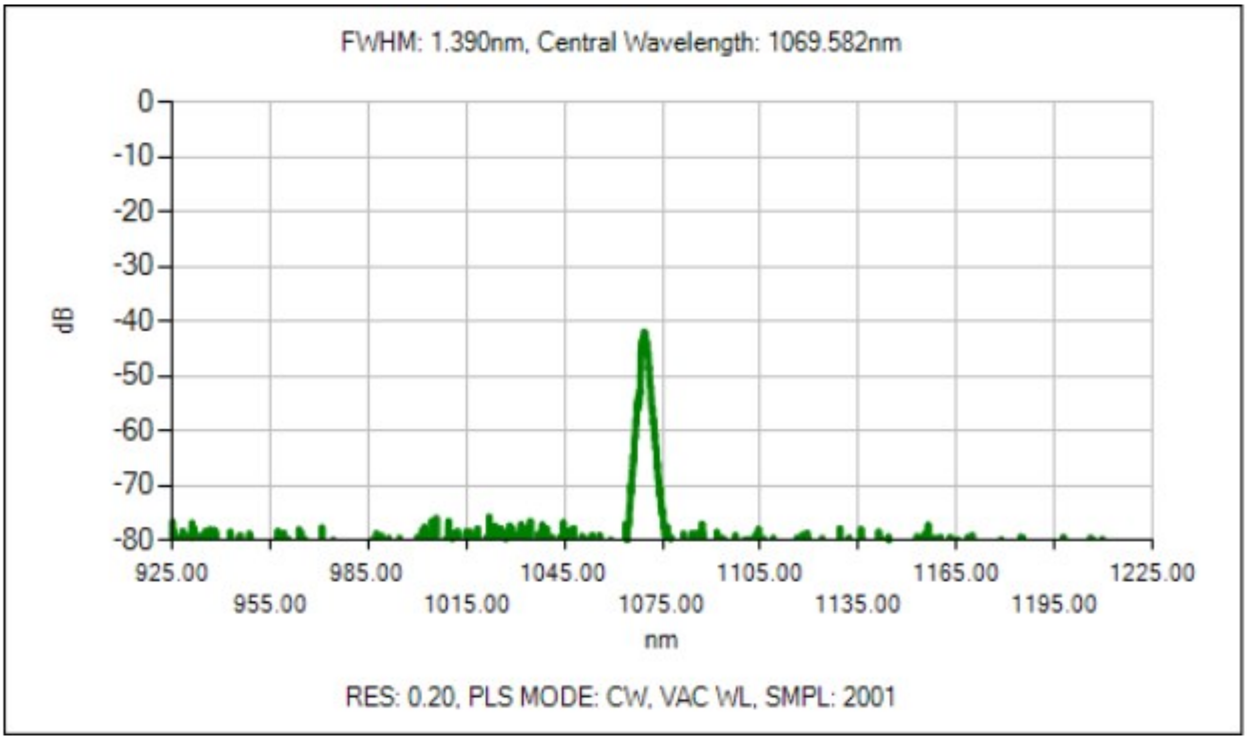

Fig. 5 Output Spectrum at Nominal Output Power

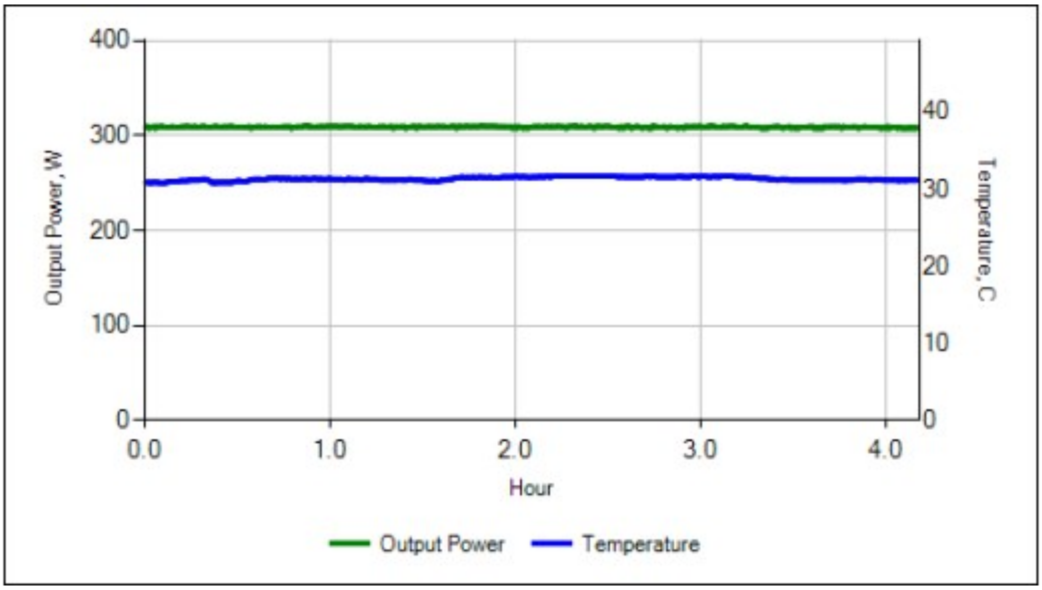

Fig. 6 Output Power Stability Chart

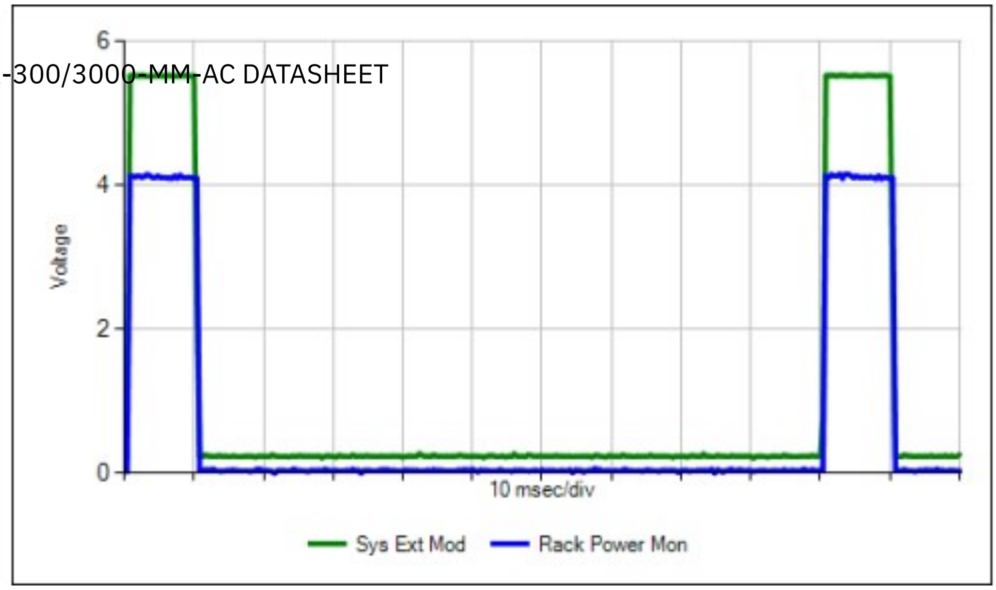

Fig. 7 Pulsed Mode: Laser Output Signal Frequency 10Hz (10% Duty Cycle)

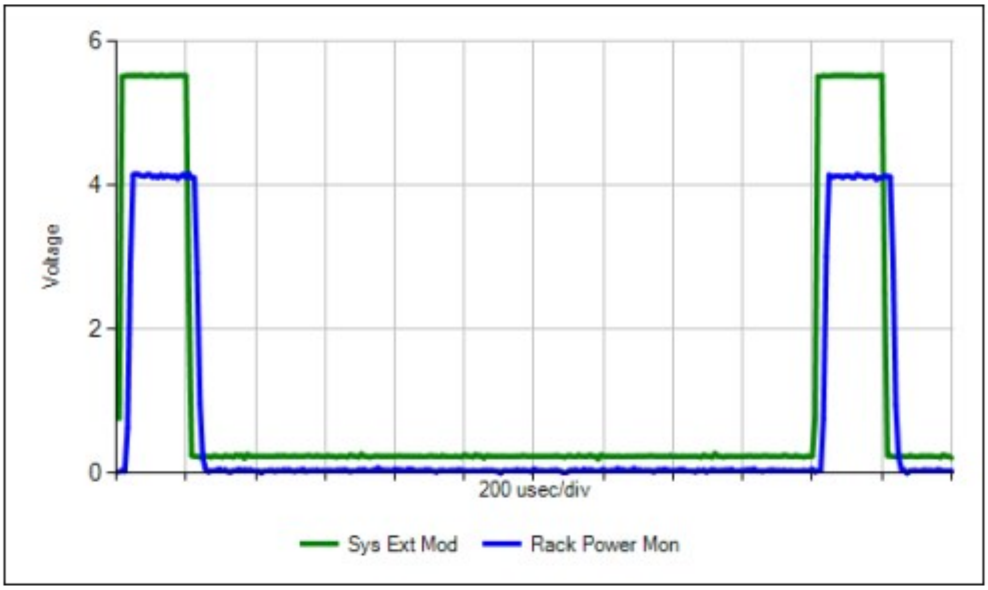

Fig. 8 Pulsed Mode: Laser Output Signal Frequency 500Hz (10% Duty Cycle)